[AMERICAN JOURNAL OF SCIENCE, VOL. 295, DECEMBER, 1995, P. 1220–1254]

SEDIMENTARY BASIN TAPER AS A FACTOR CONTROLLING THE GEOMETRY AND ADVANCE OF THRUST BELTS

STEVEN E. BOYER
Department of Geological Sciences,
The University of Washington,
Seattle, Washington 98195

ABSTRACT. **Application of the critically tapered wedge model to the study of the geometry and kinematics of thrust belts suggests spatial and temporal relationships among sedimentary basin taper (the dip of underlying basement), styles of deformation, magnitude of internal shortening, widths of thrust belts, rates of thrust-belt propagation, and the location of foredeeps. The model predicts basins or portions of basins with higher basement dips will produce thrust belts with the following characteristics: (1) fewer thrusts with larger individual displacements, (2) lower magnitude of internal shortening, (3) greater width, and (4) faster rates of frontal advance.**

Thrust belt initiation is favored in regions of maximum basement dip. As a consequence, areas of greatest crustal subsidence and the position of synorogenic depocenters will lie cratonward of regions with highest basin taper. Since the basement of most sedimentary basins is convex upward, the initial stages of tectonism should produce larger and fewer thrust sheets and result in high rates of thrust advance. As the thrust belt propagates cratonward into segments of the basin with progressively lower basement dip, the rate of thrust belt advance diminishes and the magnitude of internal shortening increases.

Lateral variations of taper within sedimentary basins should likewise affect variation in structural styles and rates of thrust belt advance in the strike dimension. Higher tapered portions of the basin initially exhibit less internal shortening and more rapid thrust advance. Lateral and cross-strike variations in basement dip produce variations in the rate of thrust belt advance and temporal changes in the geometry of the advancing thrust belt. Such structural variations, observed within Rocky Mountain thrust belts, are compatible with predictions of the critical-wedge model.

INTRODUCTION

Most thrust belts exhibit spatial variations in overall shape, thrust spacing, and internal imbrication. One example is the Cordilleran thrust belt. From southern Alberta to southern Nevada, four major salients comprise this thrust belt: (1) the Lewis salient at the United States/Canadian border, (2) the Helena embayment of west-central Montana, (3) the thrust belt of southeast Idaho, southwest Wyoming, and northeast Utah, and (4) the Provo salient to the south of the Uinta Mountains (fig. 1). Between the salients are three recesses: the Sawtooth Range thrust belt of northwest Montana, the region of southwest Montana and southeast Idaho bordering the Snake River Plain, and the small recess at the west end of the Uinta Mountains. Viewed in isolation, the Sawtooth

Range is a thrust salient, but it developed in a recess between the Lewis salient to the north and the Helena salient to the south.

Workers in the Rocky Mountains have long noted the correlation between the prominent recesses and salients of Cretaceous and early Tertiary thrust belts and the geometry of Proterozoic and Paleozoic sedimentary basins (Horberg, Nelson, and Church, 1949; Beutner, 1977). As reviewed by Grubbs and van der Voo (1976) and Beutner (1977, fig. 7, p. 361), there is no shortage of theories to explain the geometry of the thrust salients and recesses: (1) variable tectonic shortening along strike (Gwinn, 1967), (2) intersection of convergent or divergent transport directions (Rodgers, 1970), (3) oroclinal bending, (4) radially divergent gravity sliding (Crosby, 1969), and (5) impingement of eastward directed thrusts against west-directed or stationary basement buttresses (Horberg, Nelson, and Church, 1949; Crosby, 1969; Grubbs and van der Voo; 1976, Beutner; 1977). In this paper I share with Beutner the goal to demonstrate that "... the sinuosity of this segment [of the thrust belt] ... is a consequence of interaction between ... the thrust belt and geometric and stratigraphic irregularities of the craton margin ..." Beutner (1977, p. 353). However, I will not treat basement highs of the structural recesses as "buttresses" in the classical sense but will focus instead on a factor that has not received adequate attention, the primary taper of the precursor sedimentary basin (that is, the pre-deformational dip on the foreland basement).

Comparison of thrust spacing and overall shortening also serve to highlight structural variation within thrust belts. For example, the Sawtooth thrust belt in Montana has a maximum width of 28 km and contains 15 to 20 closely spaced imbricate faults (Mudge and Earhart, 1983), whereas the Wyoming thrust belt is approx 145 km wide and generally consists of 4 or 5 major thrusts exhibiting only minor internal imbrication (Royse, Warner, and Reese, 1975; Dixon, 1982; Coogan, 1993). Imbricated Paleozoic carbonate rocks of the Sawtooth thrust wedge are back-rotated and in some cases are vertical to slightly overturned, whereas in Wyoming and Idaho thrusts have low-angle trajectories and show only minor post-emplacement folding or rotation.

There are also differences in relative thrust timing among thrust belt segments. Synchronous thrusting occurs within the Sawtooth Range (Boyer, 1986, 1992), whereas the Wyoming thrust belt appears to have developed generally in a relatively simple, hinterland-to-foreland sequence, with the exception of relatively minor out-of-sequence imbrication and reactivation of existing thrusts (Royse, Warner, and Reese, 1975; Lamerson, 1982; Woodward, 1987; Coogan, 1993).

Even within the Idaho-Utah-Wyoming thrust belt there is considerable variation in structural style and the magnitude of internal shortening (fig. 2). Thrust sheets are much more internally imbricated in the northern segment of the Idaho-Wyoming thrust belt than in the southern portion (compare cross sections by Royse, Warner, and Reese, 1975; Lamerson, 1982; Dixon, 1982; Delphia and Bombolakis, 1988; and

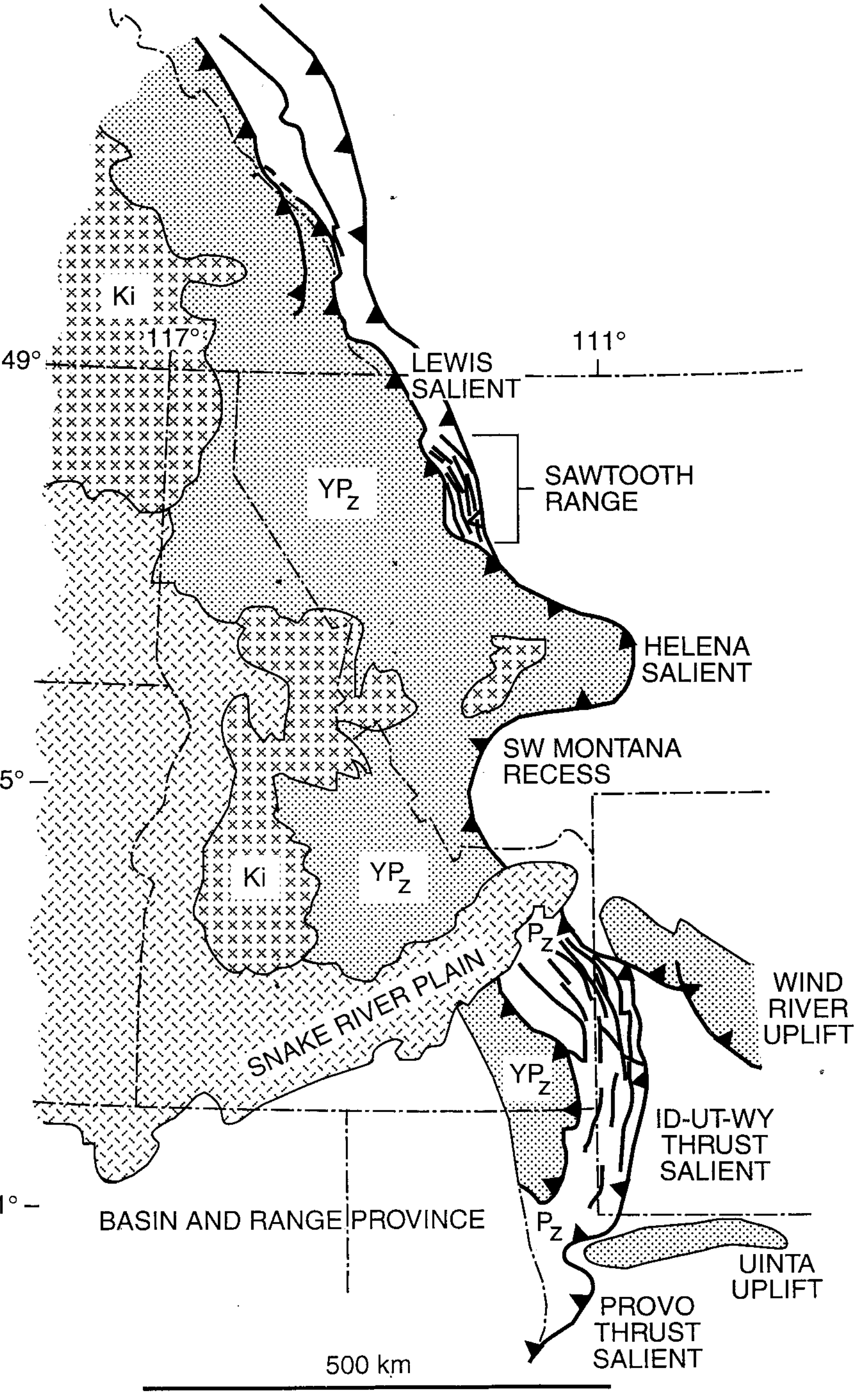

Ki
117°
49°
111°
LEWIS
SALIENT
SAWTOOTH
RANGE
YP$_z$
HELENA
SALIENT
SW MONTANA
RECESS
45°
Ki
YP$_z$
P$_z$
SNAKE RIVER PLAIN
WIND
RIVER
UPLIFT
YP$_z$
ID-UT-WY
THRUST
SALIENT
41°
BASIN AND RANGE PROVINCE
P$_z$
UINTA
UPLIFT
PROVO
THRUST
SALIENT
500 km

Figure 1

Royse, 1993). Thrust timing and frequency of out-of-sequence thrusts are variable, although out-of-sequence imbricates are for the most part limited to thrust ramps (Delphia and Bombolakis, 1988).

Similar variations in styles of internal deformation, magnitude of tectonic shortening, and thrust sequence, noted in various thrust belts and observed in experimental models, have been attributed to various factors: variations of thickness and lithologic character of the stratigraphic sequence (Woodward, 1988; Woodward and Rutherford, 1989; Marshak, 1988; Thomas, 1990; Marshak, Wilkerson, and Hsui, 1992); impingement against existing basement uplifts (Horberg, Nelson, and Church, 1949; Beutner, 1977; Kopania, 1983); effects of dewatering and lithification as sediments are deformed and incorporated into the thrust wedge (Zhao and others, 1986); and material properties considerations such as rheology of stratigraphic units and faults zones rocks, fluid pressures within the thrust wedge, and fluid pressures along the basal detachment (Davis and Engelder, 1985; Mulugeta, 1988; Colletta and others, 1991; Liu and Dixon, 1991; Calassou, Larroque, and Malavieille, 1993). Boyer (1991) proposed yet another cause for such structural variation: the effect of pre-deformational basement dip, or "basin taper."

A link between basin taper and the internal shortening, width, and propagation rate of thrust belts is implicit in the critically-tapered wedge model (Davis, Suppe, and Dahlen, 1983; Dahlen, Suppe, and Davis, 1984; Dahlen, 1984, 1988, 1990; Dahlen and Suppe, 1988) and has been employed to explain the structural variation and kinematics of the foreland fold-and-thrust belt of Pakistan (Jaumé and Lillie, 1988; Lillie and others, 1987). One paradox of the critically tapered wedge model is the rarity of hinterland internal shortening, out-of-sequence thrusting, and other mechanisms of sufficient magnitude to maintain the critical taper required of the model (Woodward, 1987). Treating the accreted sediments as a sedimentary prism, rather than a package of constant thickness, eliminates or reduces this paradox and leads to one possible explanation for the structural diversity within and among thrust belts (Boyer, 1991).

APPLICATION OF CRITICALLY-TAPERED-WEDGE MODEL TO SEDIMENTARY PRISMS

From the time of the first sandbox experiments (Cadell, 1988) the geometry, vergence, and symmetry of thrust faults and folds have driven

---

Fig. 1. The general configuration of the Cordilleran thrust belt from southern Alberta to central Utah. Middle Proterozoic through early Mesozoic sedimentary basins controlled the distribution of thrust salients and recesses. The Sawtooth Range thrust belt developed within an earlier recess between the Lewis and Helena salients. Internal complexities and structural variation within the Idaho-Utah-Wyoming thrust salient are illustrated in figure 2. Barbed lines denote the thrust front and the leading edge of dominant thrust sheets dominated by Proterozoic metasedimentary rocks. Unornamented lines are major thrusts involving Paleozoic rocks. Extensional faults not shown. Proterozoic metasedimentary and Archean basement in light stipple; Neogene plateau basalts in dark stipple. Ki denotes Cretaceous intrusives. Dashed line indicates eastern limit of Basin and Range Province. Modified from Bayer (1983).

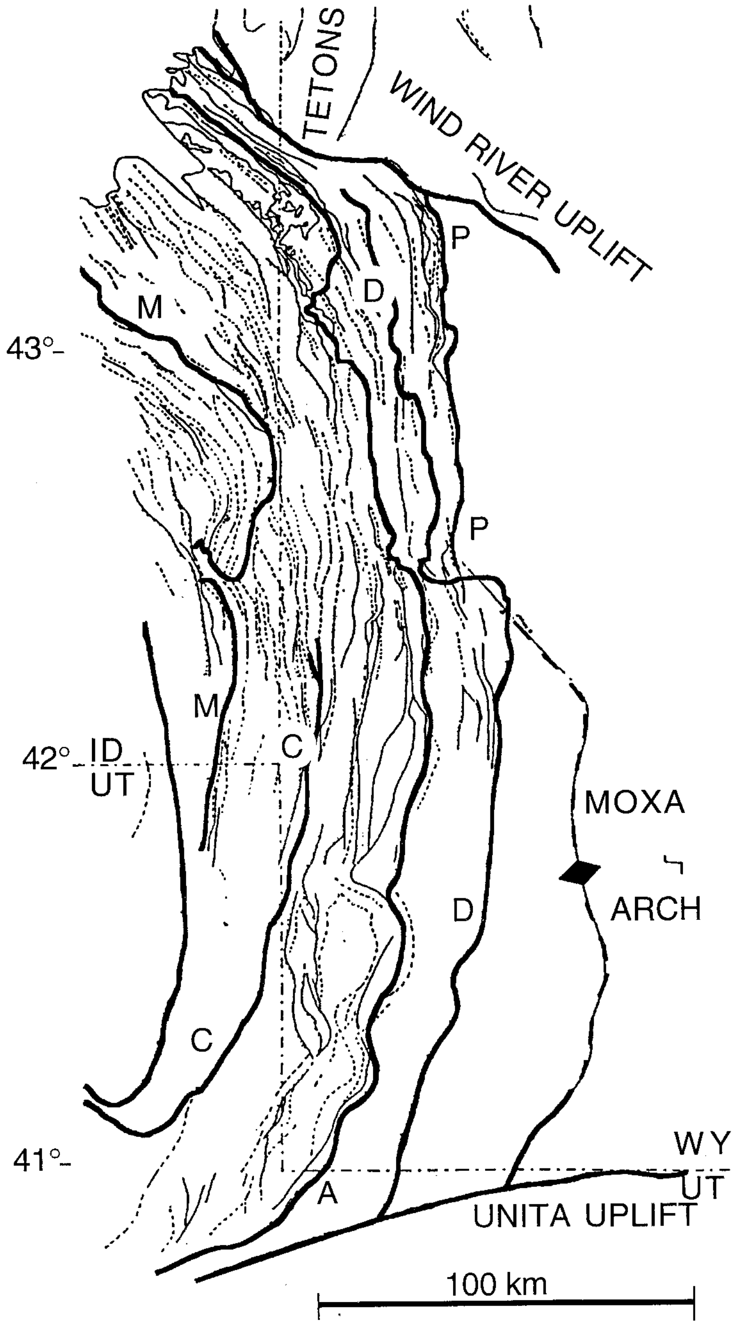
TETONS
WIND RIVER UPLIFT
P
D
M
43°
P
M
C
42°
ID
UT
MOXA
ARCH
D
C
41°
WY
UT
A
UNITA UPLIFT
100 km

Figure 2

many structural geologists to secretly favor "The Push" as the driving force of thrust belts, even though mechanical constraints indicated that gravity should play the dominant role (Elliott, 1976; De Jong and Scholten, 1973, and various references cited therein). It has been argued that the sedimentary rock packages are too weak to permit the emplacement of large thrust sheets under horizontal compression. Most thrust sheets are less than 6 km thick. However, at a fluid pressure to overburden ratio, λ, of 0.6 to 0.7, a thrust sheet of greater than 50 km width must exceed 6 km to be emplaced by horizontal compression (Hubbert and Rubey, 1959, table 1, p. 144). Only at very high pore fluid pressures ($\lambda = 0.9$) can thinner thrust sheets of these dimensions be emplaced. Since very large thrust sheets, such as the Lewis at 100 km wide (Yoos and others, 1991, fig. 3), attained much greater widths, gravity sliding was considered the only viable explanation for the emplacement of large thrust sheets. However, "The Push" returned to favor with the "critical taper" wedge model of Davis, Suppe, and Dahlen (1983).

Davis, Suppe, and Dahlen (1983) noted a weak point in the model of Hubbert and Rubey (1959): thrust sheets had been treated as tabular bodies, although they are actually wedge-shaped. Price (1973), Elliott (1976), and Chapple (1978) also entered the wedge geometry of thrust belts into their models of thrust sheet emplacement; however, in the Elliott and Price models the motive force was topography-induced gravity spreading (see physical models by Bucher, 1956). In their compressional model, Davis, Suppe, and Dahlen (1983) employed a Mohr-Coulomb failure criterion to the creation of a critically tapered wedge. However, Chapple's model and the models of Stockmal (1983), Emerman and Turcotte (1987), and Fletcher (1989) present critical taper models not restricted to a Coulomb failure criterion. For the sake of simplicity, I will present my theory of structural variation within the context of the Coulomb-based theory of Davis, Suppe, and Dahlen (1983). However, this theory should be tested further for compatibility with critical taper models invoking other rheologies.

According to the critically tapered wedge model, a thrust belt can advance under the force of horizontal compression if the taper angle, the forward dip of the topographic surface plus the hindward dip on basement, is of sufficient magnitude. This taper angle is a function of fluid pressures along the sole thrust and within the body of the thrust wedge, basal friction, angle of internal friction, and the orientation of the principal stresses with respect to the basal sliding surface (Davis, Suppe, and Dahlen, 1983).

Fig. 2. Structural complexity within the Idaho-Utah-Wyoming thrust belt increases northward. Four major thrust sheets, the Paris-Willard (PW), Crawford (C), Absaroka (A), and Darby (D), make up the southern part of this salient, whereas the dominant sheets to the north are the Meade (M), Absaroka (A), Darby (D), and Prospect (P). Heavy solid lines: major thrusts. Light solid lines: minor imbricate thrusts. Dashed lines: crestal- and trough-line traces of folds. Intra-plate imbrication and folding are more common in the north. Simplified from Blackstone and De Bruin (1987).

Theoretically, a thrust wedge can build and maintain critical taper by a combination of out-of-sequence thrusting, synchronous thrusting, underplating (duplex imbrication), and back rotation (Boyer and Geiser, 1987; Platt, 1988). Such mechanisms have operated to varying degrees in many thrust belts and accretionary prisms (Boyer, 1986, 1992, 1993; Vergés and Muñoz, 1990; Crider and Boyer, 1993; Delphia and Bombolakis, 1988; Puigdefàbregas, Muñoz, and Vergés, 1992) and have also been observed in experiments (Mulugeta, 1988; Dixon and Liu, 1992; Huiqi, McClay, and Powell, 1992). However, these modes of wedge thickening may or may not be a consequence of the critical-wedge model. The key questions in evaluating the critical wedge model are: (1) how much internal deformation is required by the model, and (2) are internal deformation and this magnitude observed (Woodward, 1987)? The answer in part lies with the relationship between thrust wedge taper and the taper of the pre-cursor basin into which the thrust belt advances.

Critical-taper models (Davis, Suppe, and Dahlen, 1983) describe wedge shapes that permit the growth and advance of thrust belts. For a given basal slope β, the required minimum surface slope α depends upon the yield envelopes for both the wedge and its base, as well as the magnitude of pore fluid pressures. The theoretical relationship between basal dips and possible surface slopes is complicated (Dahlen, 1984), but within a range appropriate to natural thrust belts the minimum taper closely approximates the form: $\alpha = \alpha_0 - m\beta$. For a dry cohesionless sand wedge on a mylar base, Davis, Suppe, and Dahlen (1983) calculated:

$$\alpha = 5.9° - 0.66\beta. \tag{1}$$

They also found that this equation agrees well with experimentally determined relations (Davis, Suppe, and Dahlen, 1983, fig. 8, p. 1160; reproduced in fig. 3 of this paper).

These relations are likely to apply to many natural thrust belts, but the presence of a weak décollement, due to elevated pore pressure or presence of ductile salt, has frequently produced narrower tapers. However, for the purpose of simplicity, I will assume that relations in many thrust belts can be approximated by eq (1). The exact values of the coefficients are less important than the fact that changes in basal dip produce geologically important effects, described below.

Assuming that this equation holds for very large values of basal slope, $\beta > 6°$, sedimentary basins with tapers of 9° or larger are at critical taper; the corresponding value of surface slope is $\alpha = 0°$. Thus, it is theoretically possible for critically and supercritically tapered sedimentary prisms to detach from their basements and advance as single coherent thrust sheets (fig. 4C). However, if the taper of the basin is subcritical the sedimentary prism will internally imbricate to build taper before the sedimentary package can advance as a thrust wedge (fig. 4A and B).

The amount of internal deformation required to build critical taper can be estimated (app. 1). It is assumed that this deformation is distrib-

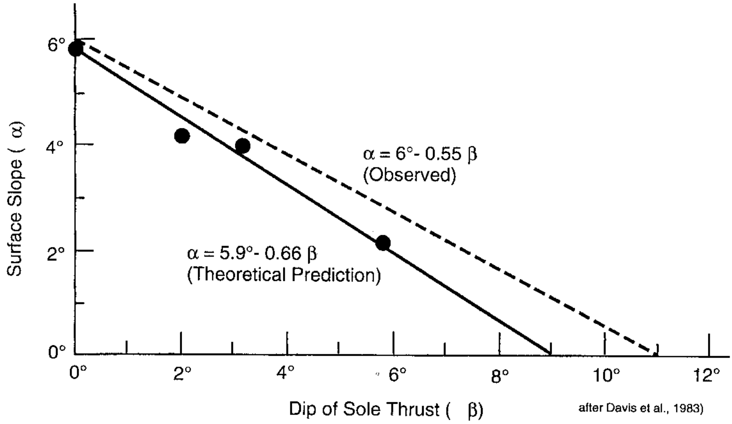

Fig. 3. Structural variation in the Rocky Mountains (figs. 1 and 2) may have been controlled in part by pre-deformational dip on the basement of Middle Proterozoic through Jurassic depositional basins. The mechanical model of Davis and others (1983) predicts that in order to build and maintain critical taper, deformation within a thrust wedge will create a topographic slope, α. All other factors being equal, α varies inversely with the dip, β, of the sole thrust (generally the dip on the underlying basement). The straight line is the theoretical prediction for a non-cohesive Coulomb material, and the four data points are from sandbox experiments (Davis and others, 1983, fig. 8, p. 1160).The dashed line is an average of a number of observed relations in thrust belts (Davis and others, 1983, fig. 17, p. 1168).

uted homogeneously throughout the thrust wedge, and that the affects of erosion and tectonic loading have been ignored. Consider a basin whose primary taper angle is β_0. Before the sedimentary prism can advance as a thrust wedge it must build taper to a critical value, τ. In doing so, the rocks of the sedimentary prism will experience tectonic strain. We can quantify this strain as a vertical extension (or thickening) at the back of the wedge (VE), horizontal shortening within the wedge (HS), or as an axial ratio strain (AR). From app. 1,

$$VE = (\tan \tau / \tan \beta_0)^{1/2}, \tag{2}$$

$$HS = (\tan \beta_0 / \tan \tau)^{1/2}, \tag{3}$$

and

$$AR = (\tan \tau / \tan \beta_0). \tag{4}$$

Figure 5 illustrates these relations in graphical form.

It should be noted that eq (1) is based on the assumption that the thrust wedge is composed of materials that behave according to Mohr/Coulomb relations. However, eqs (2-4) are not directly dependent on any assumptions concerning material properties. These equations are simply area-balance relations dictated by a given critical taper angle, which must be independently derived by either empirical or theoretical means. The

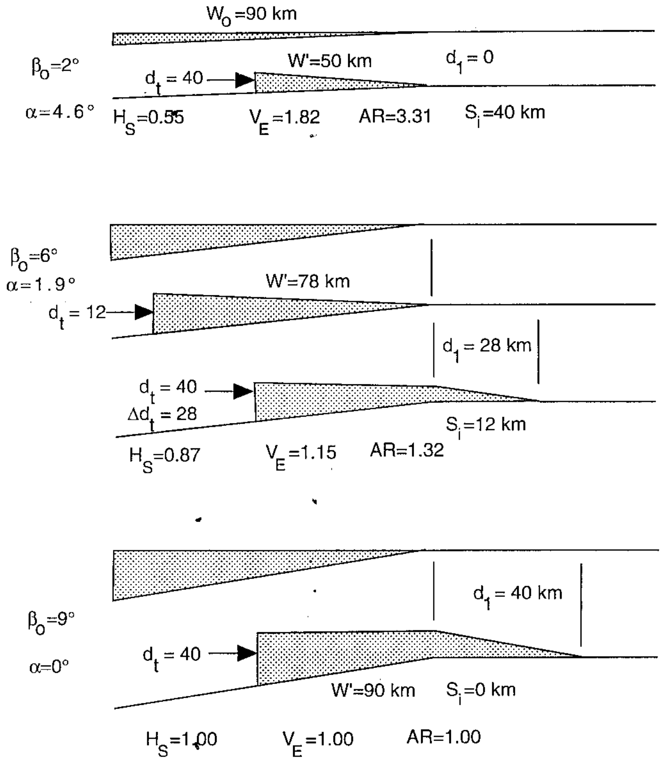

Fig. 4. Thrust-front advance for basin tapers of $\beta_0 = 2°$, 6°, and 9°. Trailing-edge displacement, d_t, that is, the translation at the back of a thrust wedge, is absorbed cratonward by the internal horizontal shortening, S_i, required to build taper. The difference between the trailing-edge displacement and internal shortening equals the advance of the thrust front or "leading-edge" displacement, d_l. H_s is the amount of internal shortening as a ratio of original thrust belt width, w_0, divided by the deformed width, w′. V_E is the vertical stretch, given by present height at the back of the thrust wedge divided by the original height prior to deformation. AR is the axial ratio of strain, given by V_E/H_s.

(A) For a basement dip of 2°, all translation at the back of the wedge is absorbed in building critical taper. There is no frontal advance of the thrust front relative to the basin margin.

(B) On a basement of 6° more of the trailing edge displacement is available for frontal advance. Twelve km is absorbed in internal shortening, while the remaining 28 km is employed in frontal advance of the thrust belt.

(C) On 9° basement, no internal deformation is required to build taper. The sedimentary prism is stripped from its basement as a single thrust sheet, a "dominant" sheet in the usage of Boyer and Elliott (1982). All tectonic input translates into frontal advance of the thrust belt.

graph of relations 2 through 4 (fig. 5) covers a range of critical taper angles, 2° to 30°.

For example, compare two sedimentary prisms, one with an initial taper of 3° and another with taper of 6° (fig. 6). Such wedges fall within the field of the Himalaya and Taiwan thrust belts (Davis, Suppe, and

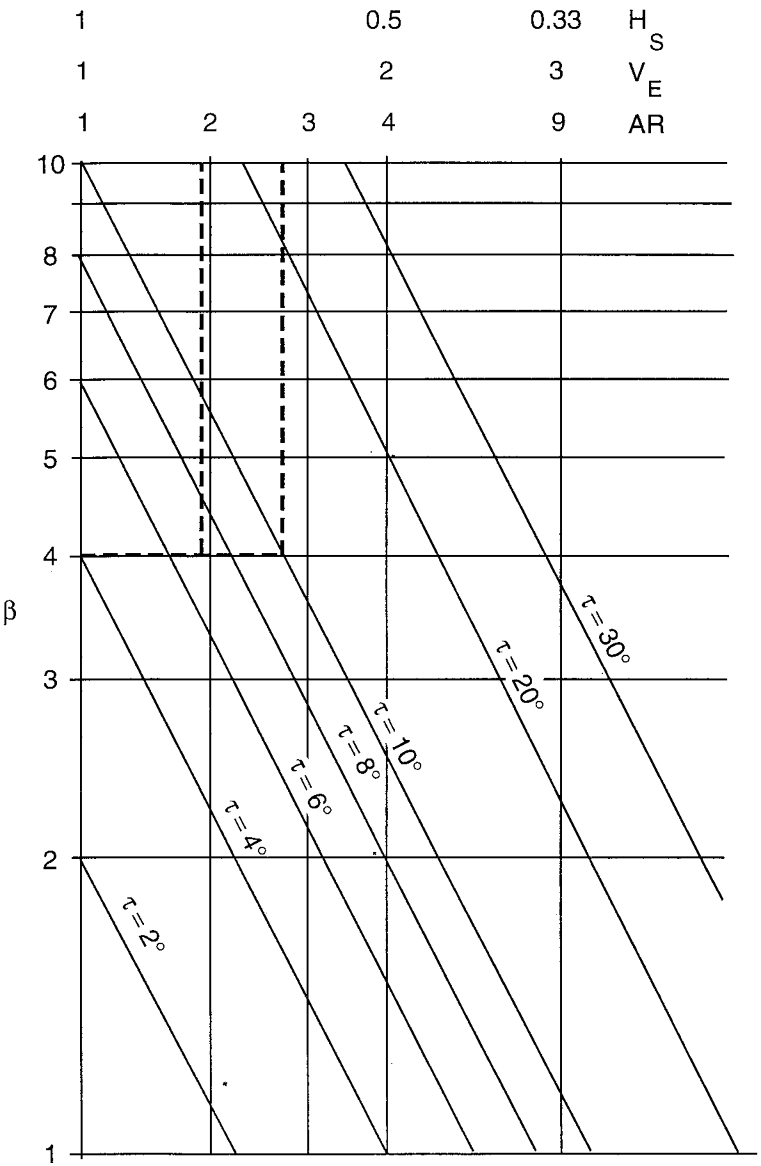

Fig. 5. As a thrust front propagates across a sedimentary prism the amount of internal deformation required to build critical taper will be a function of basement dip (see figs. 3 and 4). "AR" = average axial ratios of plane strain, "V_E" = vertical extension, and "H_s" = internal horizontal shortening. For example, if the basement dip is 4° and the rock package is behaving as a Coulomb material, one can calculate from the relation of Davis and others (1983) (see fig. 3 above) that the internal deformation will be such to create a topography of a = 3°. The critical taper, $\tau = \alpha + \beta$, will thus be 7°. Following the dashed line upward from the intercept of $\beta = 4°$ and $\tau = 7°$, one reads the average strain is approx 1.9:1. If the basal coefficient of friction is higher than for the apparatus of Davis, Suppe, and Dahlen (1983), such that the critical taper, τ, is 10°, the internal strain will be higher, approx 2.8:1. All other factors, the amount of strain within the thrust belt will decrease with increasing β.

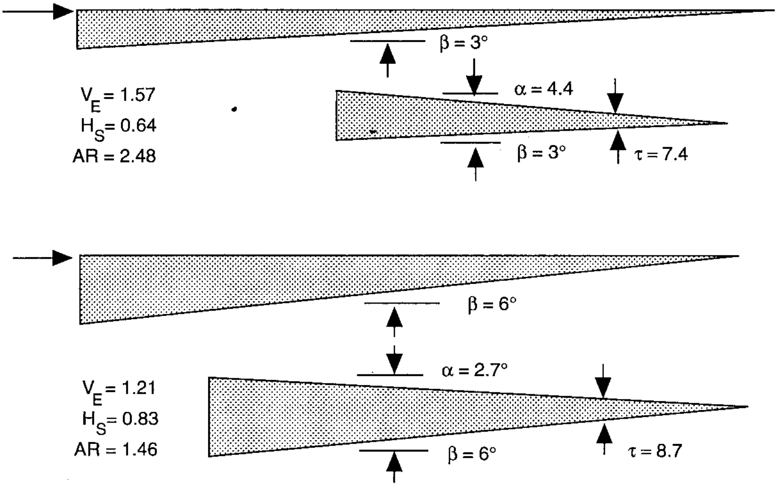

Fig. 6. Compare two sedimentary prisms with initial basement dips of 3° and 6°. What would be the internal deformation imposed upon these sediments as the thrust front swept across these two basins? I assume that the material properties and fluid pressures are such that the relationship between topography and basement dips is defined by $\alpha = 6 - 0.55\beta$ (fig. 3). From the equations in app. 1 or from the graph of figure 5, the sediments of the 3° basin would experience an average strain of 2.5:1 as they were telescoped into a critically tapered wedge. The sediments of the 6° basin would be transformed into a tapered wedge at much lower strains, approx 1.5:1.

Dahlen, 1983; 1987, fig. 17, p. 1168). Deformation would need to be of sufficient magnitude to create a 4.4° topographic dip above the 3° basement and 2.7° topographic dip above the 6° basement (fig. 3). In building the 7.4° wedge, the 3° sedimentary prism shortened internally by a factor of 0.6, with an average strain of 2.5:1. However, the 6° prism attained critical taper of 8.7° at a lower shortening factor of 0.8 and a strain of 1.5:1 (fig. 5). Since the initial dip on basement beneath a sedimentary prism can thus influence cumulative shortening in the resulting thrust wedge, and since spatial variation of basement dip is likely to occur in most sedimentary basins, such variations should produce a corresponding spectrum of structural styles that would be evident in both map and cross-sectional views.

STRUCTURAL VARIATION IN THRUST BELTS

Magnitude and distribution of strain within thrust belts.—A frequent criticism of the critical-wedge model is the absence of out-of-sequence thrusting in many thrust belts (Woodward, 1987). However, many arguments requiring out-of-sequence thrusting and other taper-building mechanisms suffer from the same shortcomings as the mechanical models of Hubbert and Rubey (1959): they treat the sedimentary package as a tabular body (Dahlen, 1988; Woodward, 1987). While this may be so in some cases, most sedimentary basins and synorogenic foredeeps are wedges (Price, 1973; Royse, Warner, and Reese, 1975; and Hayes, 1977). As has been shown previously, sedimentary basin taper controls the need for tectonic taper-building mechanisms. Since most thrust belts have developed in sedimentary basins displaying a basinward increase in basement dip (pre-deformation basin taper), internal shortening may be considerably less than that required by the analysis of Woodward (1987).

Most sedimentary basins not only have a wedge shape, they are convex upward with basal slope increasing toward the deeper parts of the basin (fig. 7). {In order to analyze properly the pre-deformational shape of sedimentary basins the effects of strain must be removed (Mitra, 1993), a step that was not taken in the construction of figure 7. Therefore, the basement gradients in figure 7 constitute a maximum.} The foreland decrease in the dip of the basement surface will affect the spacing of master thrusts, the degree of internal shortening within thrust sheets, and the total shortening of the thrust belt (fig. 8).

Large sheets, "dominant thrust sheets" (Boyer and Elliott, 1982), develop in the hinterland where taper is critical to supercritical, whereas

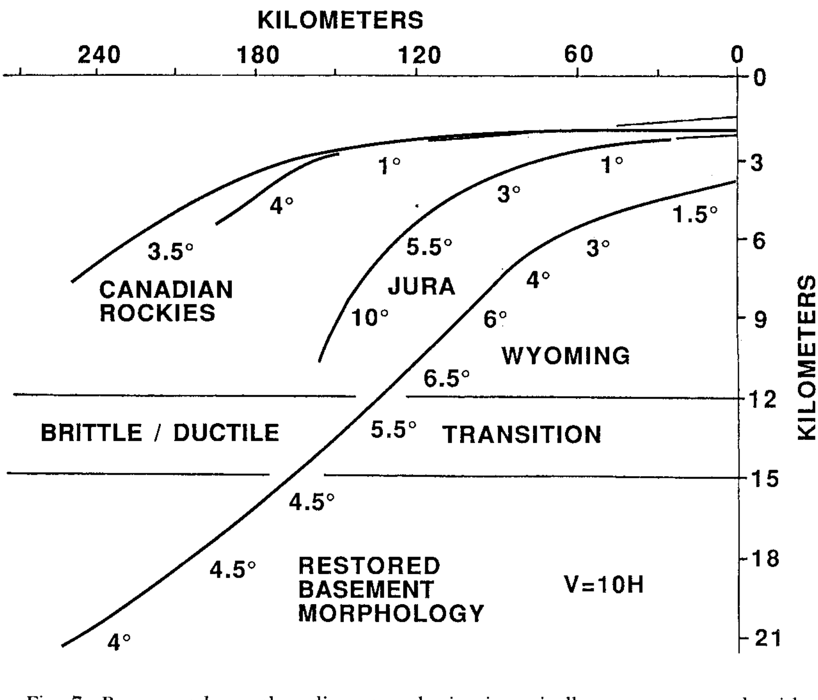

Fig. 7. Basement beneath sedimentary basins is typically convex upward, with dip decreasing cratonward. Typical basement profiles are reproduced from the Canadian Rockies (Bally and others, 1966), the Jura (Mugnier and Vialon, 1986), and the Idaho-Utah-Wyoming thrust belt (Royse and others, 1975). Such basement profiles should influence internal deformation within the thrust wedge (fig. 8).

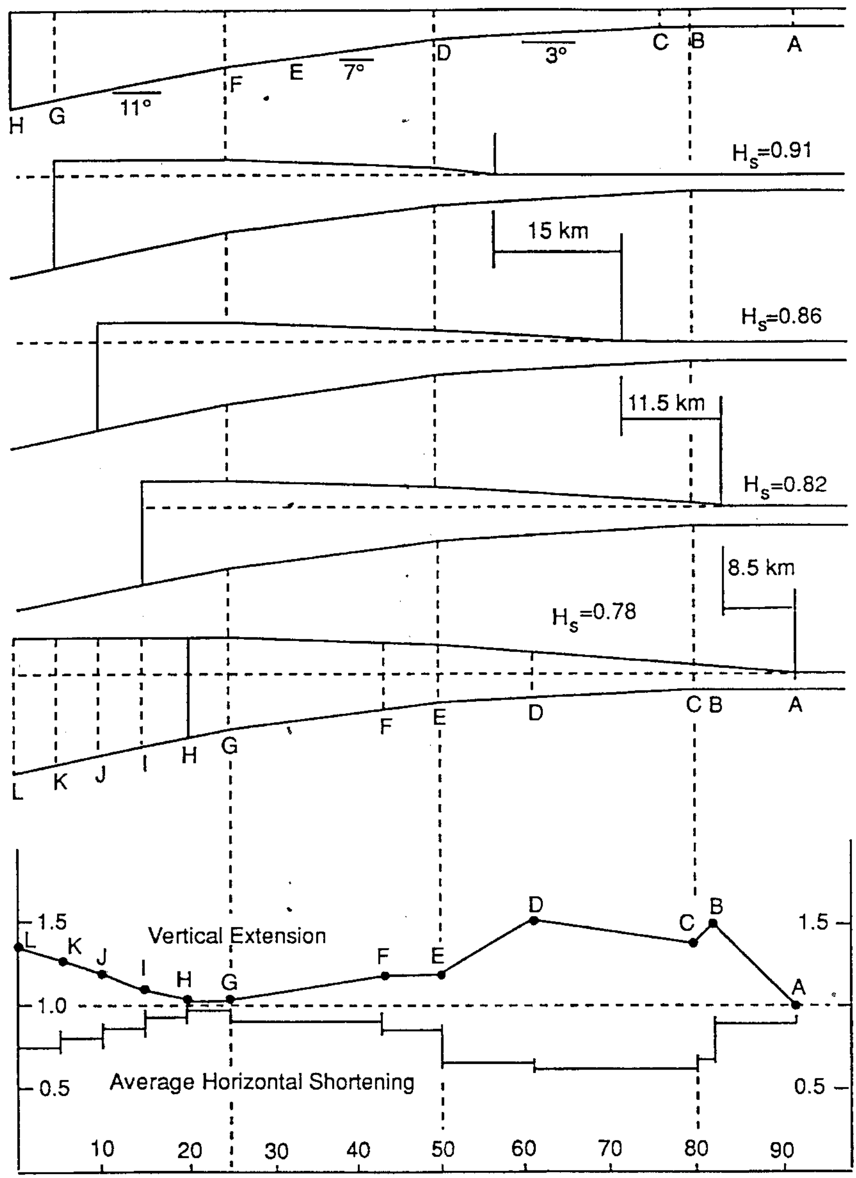

Fig. 8. The convex upward geometry of basement beneath most sedimentary basins would be expected to produce a thrust belt with a convex upward topographic profile. The creation of the critically tapered surface profile requires spatial and temporal variations in the magnitude of internal strain.

(A) The basin basement is modeled in four planar increments of 11°, 7°, 3°, and 0° to simulate a convex upward geometry. (Caption continued on facing page.)

toward the foreland creation and maintenance of taper require greater internal imbrication. Layer-parallel shortening should be greatest near the leading edge of the thrust wedge and decrease toward the foreland. For example, in figure 8, the axial ratios of strain would be the following in the vicinity of indicated references lines: 1.0 (A), 2.04 (B), 1.82 (C), 2.10 (D), 1.50 (E), 1.49 (F), 1.12 (G), and 1.12 (H). From "L" toward the remainder of the hinterland, where the sole thrust is assumed to detach near the top of the brittle/ductile transition at a depth of 12 km, the average strain would be constant at 1.88 in the final state. Should the thrust belt advance farther into the foreland, where the basement dip is 0°, strain would increase rapidly throughout the wedge, in the manner suggested by Woodward (1987).

Although thrust imbrication constitutes the greatest proportion of tectonic shortening in most thrust belts, buckle (detachment) folding and ductile strain in the form of penetrative metamorphic and pressure solution fabrics, also add to the total tectonic shortening. Pressure solution cleavage and tectonic compaction are often the first response to crustal shortening and commonly define the deformation front in thrust belts (Nickelsen, 1972, 1979; Geiser and Engelder, 1983; Protzman and Mitra, 1985; Mitra and others, 1988; Geiser, 1988a, b). Intuitively, one would expect penetrative fabrics to increase in significance toward the metamorphic core of an orogenic belt. However, the model just presented implies that penetrative fabrics should constitute a greater percentage of shortening in the foreland than in the hinterland. Since cleavage shortens and thickens the stratigraphic section, it can play an important role in building and maintaining taper. Due to higher basin taper toward the deepest part of a basin, layer-parallel shortening by penetrative deformation may be weak or absent in dominant hinterland sheets but may play an important role in shortening of sedimentary units toward the foreland where basin taper was not sufficient for thrust advance. Such layer-parallel shortening is likely to manifest itself by pressure solution

---

(B) After a hinterland displacement of 5 km, a critically tapered thrust belt has developed. The average internal shortening within the wedge, H_s, is 0.91.

(C) After an additional 5 km displacement, the thrust front has advanced another 15 km. During this time frame the average rate of frontal advance was 3 times the hinterland displacement rate. Average internal shortening has increased to 0.86.

(D) The thrust front slows as it overrode regions of lower basement dip. Displacement in the hinterland has been absorbed as strain within the thrust belt to build additional taper over low-dipping basement and is thus subtracted from frontal advance. Average horizontal shortening of 0.82.

(E) During the final 5 km displacement the thrust front has advanced onto 0°-dipping basement. With the need for internal strain to build additional taper, the rate of frontal advance has approached the value of the trailing edge advance. Average internal shortening within the entire wedge has increased to 0.78. "L", "K", "J", and "I" indicate the incremental trailing edge advances of the preceding four cross sections. Vertical material reference lines "A", "B", "C", "D", "E", "F", "G", and "H" are shown in the undeformed state (cross section A) and the final deformed state (cross section E).

The bottom figure indicates (1) the vertical extension for the reference lines "A" through "L", and (2) the average horizontal shortening within trapezoids bounded by the reference lines. The reference scale at the bottom is in kilometers.

cleavage in argillaceous limestones and by tectonic compaction in clastic units.

Convex shape of thrust belt.—Note in figure 8 that the convex shape of the basement produces a convex topographic surface in the overlying thrust belt, with a plateau uplift at the trailing edge of the thrust belt. Davis, Suppe, and Dahlen (1983) demonstrated that plateau uplifts should occur where the sole thrust merges with the brittle-ductile transition. As previously illustrated by Mugnier and Vialon (1986) and Jaumé and Lillie (1988), a hinterland increase in basement dip could produce or enhance the same effect.

Spacing of thrusts.—Thrust spacing decreases toward the foreland of most thrust belts (Goff and Wiltschko, 1992, fig. 1). As demonstrated by "sandbox" experiments and predicted by mechanical models, the thickness of the sedimentary package is a major factor controlling the spacing of thrusts (Colletta and others, 1991; Huiqi, McClay, and Powell, 1992; Marshak and Wilkerson, 1992; Marshak, Wilkerson, and Hsui, 1992). Although modeling by some workers suggests that thrust spacing will decrease cratonward even in the absence of stratigraphic taper (Goff and Wiltschko, 1992), the experiments of Huiqi, McClay, and Powell (1992) and Colletta and others (1991) clearly illustrate the role of stratigraphic thickness. Consequently, as a thrust belt propagates across a sedimentary prism, the spacing of thrusts will decrease (fig. 9).

Cross-strike variation in thrust spacing should occur over shorter distances in high-taper basins than in low-taper basins, as there is a greater cross-strike variation in the thickness of the sedimentary package. For the same reason, one would expect thrust spacing to be more uniform in low-taper basins than in basins of higher taper. Also, due to the convex shape of most sedimentary basins, cratonward decrease in thrust spacing occurs over a shorter distance in such basins than in basins of constant basement dip.

Strike-parallel structural variation.—Basement dip may vary continuously along strike or experience abrupt changes due to the presence of pre-thrust cross faults (Thomas, 1990). The area balance equations of the previous section would predict a change in internal shortening and magnitude of thrust advance related to these along-strike changes in basin taper. Lateral variations in internal shortening may be reflected not only by intensity of thrust imbrication and folding but also by the significance of penetrative mechanisms, such as pressure-solution and tectonic compaction.

In regions of low initial basin taper, 2°, internal shortening, which is required to build taper, absorbs most of the tectonic input (fig. 4A) and diminishes the amount available for thrust front advance. For a much higher basement dip, 6°, internal thrust shortening is less, and greater tectonic displacement is translated into thrust belt advance (fig. 4B). However, if the dip on the basin taper equals the critical angle for thrust advance, the sedimentary prism can be stripped from its basement as dominant thrust sheet with little or no internal deformation required to

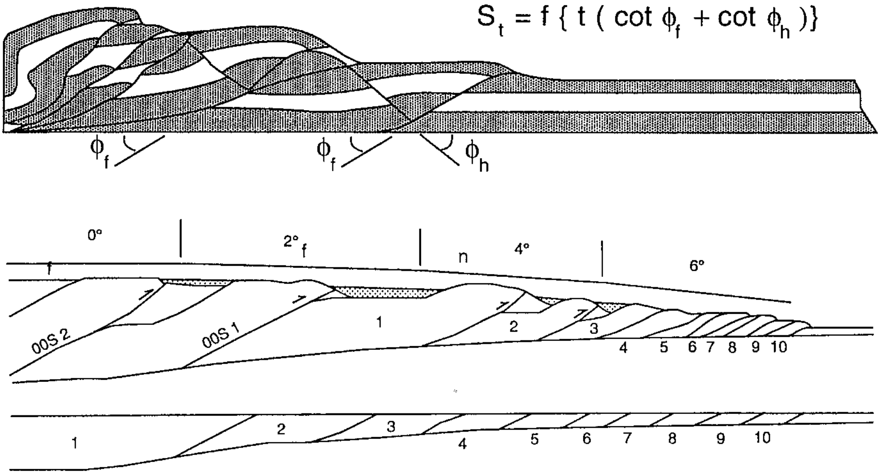

Fig. 9. Spatial variation in thrust spacing is controlled by changes in stratigraphic thickness, which is in turn a function of taper angle.

(A) In sandbox experiments the spacing of thrusts is governed by Coulomb failure angles and the thickness of the sand, **t**, (Colletta and others, 1991; Mulugeta and Koyi, 1987, 1992; and Huiqi and others, 1992). ϕ_f and ϕ_h are the dip of the foreland-vergent and hindward-vergent thrusts, respectively. At the initiation of each new imbricate the incipient backthrust dips toward the foreland from the thrust front. A new foreland-vergent imbricate propagates from the branch line of the backthrust and the basal detachment. The incipient backthrust deactivates as movement is transferred to the new thrust imbricate.

(B) A synthetic thrust belt produced over a basal detachment that decreases in dip from 9° to 0°. "OOS2" and "OOS1" are so-called "out-of-sequence" thrusts required to maintain elevation in the hinterland as the thrust belt grows in width by frontal accretion. Note the cratonward decrease in thrust spacing with decreasing dip on basement and accompanying decrease in depth to the basal detachment.

build critical taper (fig. 4C). All the tectonic shortening in the hinterland translates into frontal advance of the thrust wedge.

As an example, consider a thrust belt developed within a basin exhibiting three-dimensional variation in basement dip. Not only does total internal shortening vary transversely and longitudinally, but the spacing and displacement on individual thrusts also vary (fig. 10). At low taper, the thickness of the sedimentary package is thinner, and imbricate spacing is less. Thrust sheets are shorter, and the displacement on individual thrusts is greater than is the case on the higher taper wedge. For experimental examples, see the experiments of Colletta and others (1991) and Huiqi, McClay, and Powell (1992).

Smooth lateral variations in basement dip will produce an interweaving pattern of imbricate faults which transfer displacement between the large, continuous thrust sheets, in regions of high basin dip, and the more closely spaced and intensely shortened imbricates, in adjacent regions of low initial basin dip (fig. 10). Alternatively, very rapid lateral changes in basement taper may lead to the formation of cross-strike

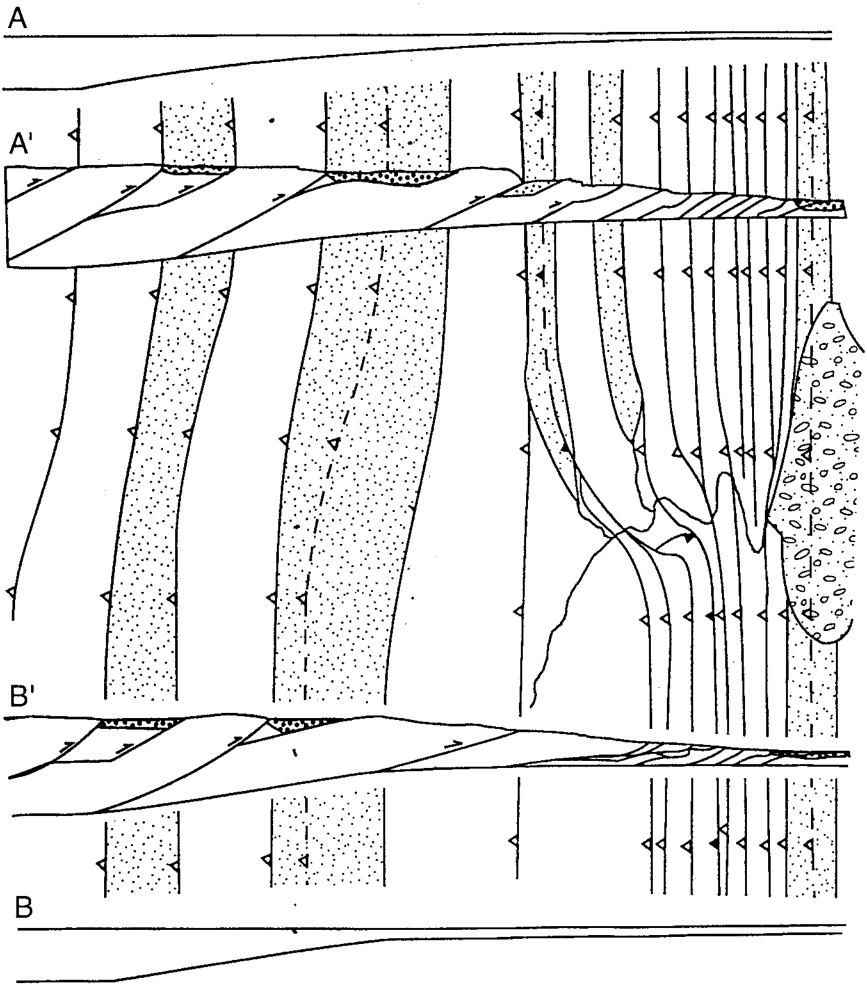

Fig. 10. Map and cross sections of hypothetical thrust belt, illustrating structural variation induced by cross-strike and strike-parallel changes in basin morphology. Thrust belt trends north-south, with north to top. In the north (A), dip on basement varies gradually from 9° to 0° over 140 km, whereas to the south (B) basement dip is 9° and decreases abruptly to 0° 70 km east of the depocenter. The deformed cross section, A′, is from figure 9. Deformed section B′ was constructed in a manner similar to the section of figure 9. Thrust symbol with blackened barbs denotes the thrust front for dominant sheets. "OOS" are minor out-of-sequence thrusts required to adjust taper during frontal accretion. Note that forward of the dominant sheets the foreland thrust belt is only 22 km wide in the south but increases northward to 65 km.

partitioning faults (Thomas, 1990; Lawton, Boyer, and Schmitt, 1994). Such variation in structural style affects sediment transport and the spacing and width of piggyback basins (Lawton, Boyer, and Schmitt, 1994).

INITIATION, ADVANCE, AND GROWTH RATE OF THRUST BELTS

Sedimentary basin taper exerts control on many aspects of the growth and advance of thrust belts: (1) the initiation of dominant thrust sheets and the locus of initial thrust advance, (2) the magnitude of shortening within the thrust wedge, (3) the spatial and temporal variation in the widths of thrust belts and thus the rates at which thrust belts grow in width, and (4) rates of thrust belt advance.

Since basement is convex upward, the initial thrust is likely to develop in the deeper parts of the basin where the dip on the basement surface is greatest and the least internal deformation is required to build taper. These initial sheets in hinterland regions can be quite large and are termed "dominant sheets" (Boyer and Elliott, 1982). Minimum-work considerations favor dominant thrusts, whose basal fault is at or near critical dip; no building of a foreland dipping topographic dip is required.

The initial width of the thrust belt, which is the width of the first dominant sheet, is determined by the trajectory of the initial thrust and the depth to the brittle/ductile transition (see app. 2). Assuming an average fault trajectory of 5° to 10° and a brittle/ductile transition at 12 to 15 km, the initial width of the thrust belt would be 65 to 170 km. For example, the Lewis thrust sheet has a width of approx 100 km (Yoos and others, 1991), which may reflect the approximate width of the northwest Montana thrust belt at its inception. I based this conclusion on the assumption that thrust faults detach on the brittle/ductile transition, an assumption that is commonly made but has yet to be proved.

As a thrust belt grows, its intermediate and final widths are a function of shortening internal to the thrust wedge and the advance of the thrust front. The greater the shortening required to build and maintain taper, the narrower the thrust belt should be in its final state (fig. 4). Throughout its development, the thrust wedge will cyclically increase and decrease in width as convergence alternately translates into: (1) propagation of the frontal thrust and (2) advance of the thrust wedge accompanied by internal shortening to maintain taper. The net result is a step-wise increase in thrust belt width (Mulugeta and Koyi, 1992, fig. 6, p. 327). However, since this paper focuses on thrust advance from the standpoint of material balance, I consider the advance of the thrust wedge to progress by continuous accretion, rather than an episodic process of thrust propagation followed by thrust wedge advance.

To visualize the effect of basin geometry, consider a basin in which the dip on basement, β_0, varies along strike from 4° to 8° (fig. 11). I assume the basin to be flat-bottomed with a maximum depth of 15 km. The sedimentary package thins to a thickness of 4 km on the "craton." The basin has upper and lower "hinge lines" between which the basement slopes basinward. The "hinge lines" intersect each cross section at "hinge points." To compare rates of advance the lower hinge points of the 4° and 8° basin segments are aligned (fig. 11A). On the basis of area balance considerations, I have calculated the width of the thrust belt for given values of displacement within the hinterland of the orogenic belt.

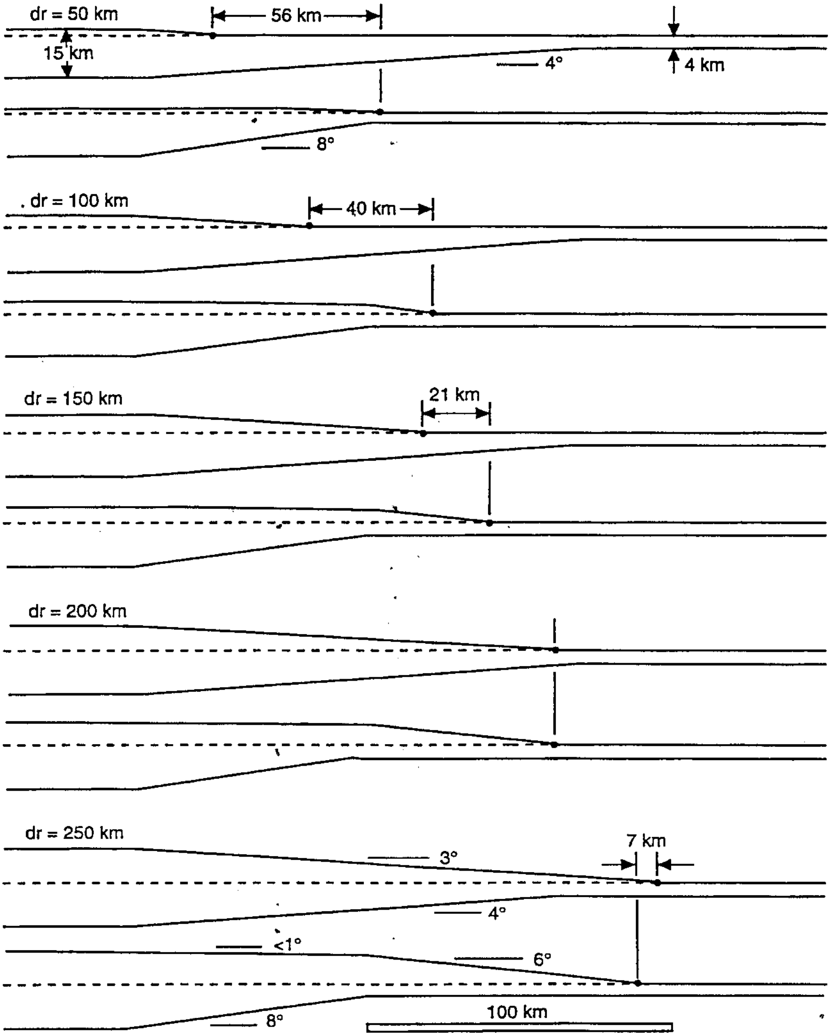

Fig. 11. A comparison of the temporal advance of two thrust belts developed over basements of dips $\beta = 4°$ and $\beta = 8°$. Five stages of deformation denoted by total hinterland displacements of 50, 100, 150, 200, and 250 km. Note that the thrust belt width is initially wider above the 8° basement, but in time the thrust belt over 4° basement "catches up."

In calculating the surface dip, α, I assumed a Coulomb material and utilized the relations of Davis and others (1983) (fig. 3). App. 2 details the construction method for the sections.

Note that the initial thrust wedge advance is fastest over the more steeply dipping basement. In regions of high basement dip less internal deformation is required to attain critical taper, and a larger percentage of tectonic shortening translates into frontal advance of the thrust belt. After an initial displacement, d_r = 50 km, within the core zone, the thrust wedge above the 8° basement is 56 km to the fore of the adjacent wedge overlying 4° basement (fig. 11A). However, as the leading edge of the thrust belt crosses the hinge line, the initial advantage, given to thrust advance in the areas of higher basement dip, is lost. Upon crossing the hinge line, the thrust wedge builds taper, through internal shortening, to compensate for the change to flat basement. Displacement at the back of the thrust wedge is thus absorbed in building taper within the thrust wedge and cannot be translated into frontal advance of the thrust belt. As a result, the thrust belt over 4° basement, which initially lagged behind, catches up with the thrust front over 8° basement (fig. 11D) and overtakes it (fig. 11E).

Note that the fully developed orogenic belt (fig. 11E) possesses a plateau uplift overlying hinterland regions where the sole thrust detached on the brittle/ductile transition (Davis and others, 1983) or basement dip approached criticality.

All other factors being equal, the rate of thrust belt advance depends upon the initial taper angle. For example, let us assume that displacement in the hinterland of 50 km (fig. 11B) took place in 25 Ma at an average rate of 2mm/yr. Over this period, the thrust belt built upon 8° basement grew to a width of 85 km. However at some distance along strike, where the dip had diminished to 1° to 2°, the thrust belt widened to only 20 km. Thus, hinterland displacement rate of 2mm/yr translates to a front advance of 3.4 mm/yr over 8° basement, whereas in the region of 1° to 2° basement dip the rate of thrust front advance is on the order of 0.8 mm/yr.

Consider a thrust belt developed within a basin of complex basement geometry and laterally varying sediment thickness (fig. 12). The apparent dip on basement is constant in dip profile and ranges between 4° and 8° (fig. 12A). Viewed in strike profile, the basin varies from convex to concave and contains a cratonal "buttress" in the "northwest" and a depocenter in the "southeast." The sedimentary package is of constant 4-km thickness on the craton and reaches a maximum of 15 km in the depocenter.

The thrust belt initiates with two prominent salients, but as the thrust front crosses the upper hinge line it slows in response to taper-building. The thrust salient opposite the cratonal buttress crosses the hinge line earlier than does the salient initiated within the depocenter. As a consequence, the former is eventually eradicated, and at the close of thrusting only one prominent salient remains (fig. 12B).

The results are somewhat different for lower dips, 2° to 6°, on basement (fig. 12C). Given the same magnitudes of orogenic translation, two distinct salients persist throughout the evolution of the thrust belt. At lower dips the distance between hinge lines is greater, and thus much

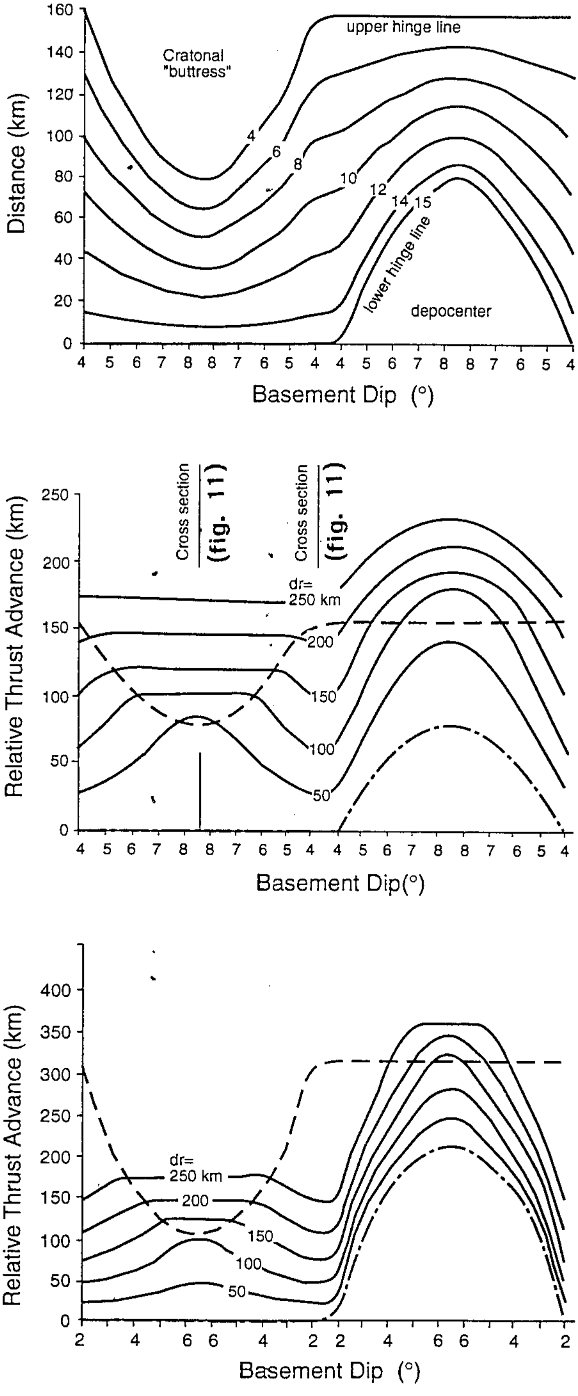

Distance (km)
upper hinge line
Cratonal "buttress"
4
6
8
10
12
14
15
lower hinge line
depocenter
Basement Dip (°)
Relative Thrust Advance (km)
Cross section (fig. 11)
Cross section (fig. 11)
dr= 250 km
200
150
100
50
Basement Dip(°)
Relative Thrust Advance (km)
dr= 250 km
200
150
100
50
Basement Dip (°)

Figure 12

greater translation is required for the leading edge of the thrust wedge to cross the upper hinge line.

Note that the "buttress" does not block thrust advance in the classical sense proposed by Beutner (1977) and others. Low dip on basement dip, rather than the barricading effect of a basement obstacle, acts to retard thrust advance.

EFFECTS OF TECTONIC LOADING AND SUBSIDENCE

The previous discussion has ignored the effects of tectonic loading. The tectonic load of one or more dominant thrust sheets will depress the foreland crust, increasing the dip on the basement and causing the foredeep to migrate cratonward (Price, 1973; Royse, Warner, and Reese, 1975; Beaumont, 1981; Jordan, 1981). The dip on the foreland crust continues to increase, as a function of tectonic load, until it reaches a critical value. Then the next thrust initiates. Thus thrust advance can be a self-perpetuating process: the advance of the initial dominant sheet increases basin dip, which favors the initiation of the next thrust (fig. 13). Subsidence of the crust is not only a *response* to thrust belt advance, it is the *facilitator* of such advance.

This feedback loop between basement dip and thrust advance leads to rapid thrust advance in regions of maximum basement dip and produces prominent thrust salients. For example, the geometry of an aulacogen in the Middle Proterozoic Belt/Purcell basin controlled formation of the Helena salient (fig. 14A) (Winston, 1986; Harris, 1957; Harrison, Griggs, and Wells, 1974). On the basis of the model just presented, I propose that the Lewis and various sheets carrying Belt/Purcell rocks in the Helena embayment advanced by virtue of their great thickness and primary taper. These dominant sheets loaded and depressed the crust, leading to the formation of additional sheets and the advance of the thrust belt to create the Lewis and Helena thrust salients.

As the thrust belt advanced into regions of lesser basement dip and the thrust front crossed the hinge line, the thrust fronts within the Lewis and Helena salients may have slowed by the need to build taper. Thus,

---

Fig. 12. Thrust front advance as a function of basin morphology. Distance scales vary on the three figures.

(A) Contour map of depth to basement within a complex basin. Distance scale along "Y" axis. Dip on basement varies along strike, that is, along the "X" axis, but is constant along the "Y" axis. Contours in kilometers. Above upper hinge line basement considered to be planar at depth of 4 km. Below lower hinge line basement is planar at depth of 15 km. This basement configuration is used to model thrust front advance (**B**).

(B) Thrust front advance in a basin with the configuration shown in (**A**). The dashed line indicates the position of the upper hinge line, and the dot-dash line shows the position of the lower hinge line. The solid lines display the position of the thrust front after trailing edge displacements, dr, of 50 to 250 km. Note changing shape of the thrust front with increasing displacement.

(C) Thrust front advance over complex basin with dips of 2° to 6° on basement. Compare with (**B**), where the dips varied between 4° and 8°. Due to the lower dips on basement the hingeline is not crossed until later in the thrust front advance, thus resulting in the retention of a more prominent thrust salient than was the case in model (**B**).

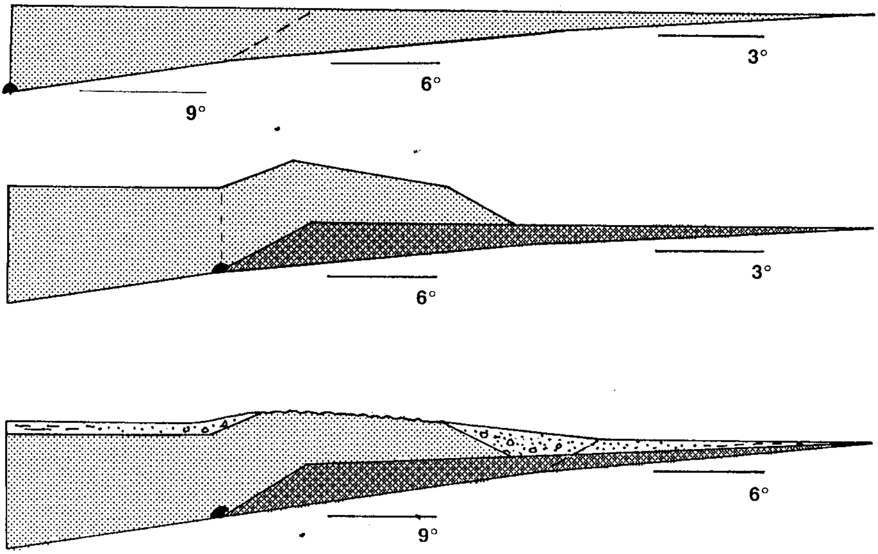

Fig. 13. Initiation of dominant thrust sheets in regions of high basin taper can be a self-perpetuating process.

(A) Consider a basin, viewed in cross section, in which the basement dip decreases in convex fashion from 9° in the hinterland to 3° in the foreland. The convex geometry has been modeled as three panels of basement dip: 9°, 6°, and 3° dip.

(B) A thrust is most likely to initiate in the region of maximum basement dip, as less internal deformation is required to build taper, and thus the least amount of work will be expended.

(C) The tectonic load of the initial sheet depresses the crust, bringing additional portions of the foreland basement to critical taper, thus leading the initiation of the next thrusts.

the Sawtooth thrust belt of the Sawtooths caught up with the thrust front of the Lewis thrust, but the thrust salient developed within the Helena embayment was able to maintain its dominance throughout the evolution of the thrust belt.

Similar relationships among Proterozoic/Paleozoic sedimentary basins, crustal subsidence, and thrust belt advance exist in the Idaho-Utah-Wyoming thrust belt and the Provo thrust salient of central Utah (fig. 15). Depocenters for the synorogenic sediments lie due east of the depocenters of Paleozoic deposition. In accord with the model just presented (fig. 13), I would argue that the initial master thrust sheets developed near the center of the Paleozoic basins where the thickness of the sequence and the dip on underlying basement were the greatest. Due to high basement dips, the initial sheets would have developed on the steepest dipping flanks of Paleozoic depocenters where the need for the creation of topographic taper would have been the least. As these dominant sheets advanced they loaded the foreland. The thrust load increased the dip on the foreland basement, which in turn led to the

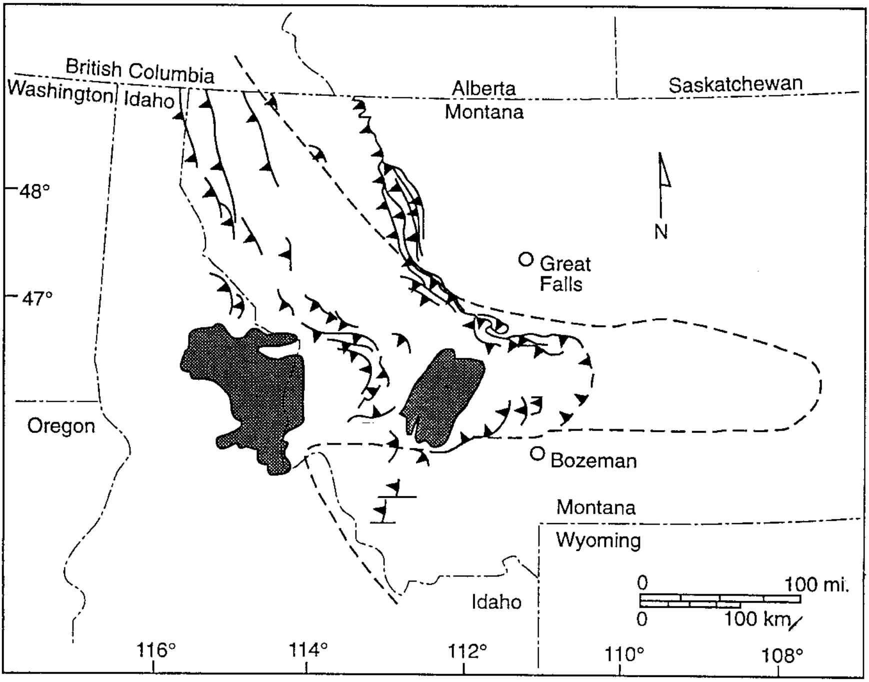

Fig. 14. The dip of basement and thickness of Proterozoic/Paleozoic sedimentary rocks within the Helena embayment may have controlled the geometry of the associated thrust salient and the spacing of thrusts within the salient. Barbed symbols indicate major thrusts. Shaded areas are Idaho Batholith (to west) and Boulder Batholith (to east). The dashed line shows the approximate eastern limit of Proterozoic Belt/Purcell metasedimentary rocks and thus defines the gross geometry of Belt/Purcell basin. Modified from Winston (1986).

development of the next thrust sheets to the east. Thus the areas of thrust belt initiation, controlled by initial basement dip, became the loci of most rapid thrust advance.

To the north and south of the Paleozoic depocenters and subsequent foredeep basins, the initial dip on basement was subcritical, and greater deformation was required to create critical taper. This enhanced deformation and associated uplift fed increased erosion. The resulting synorogenic sediments would have been transported along-strike into the foredeeps.

Erosion may counter or moderate the effects of tectonic loading and subsidence discussed previously. Erosion leads to isostatic adjustments that decrease the dip on basement. Consequently, α and β decrease, and restoration of critical taper requires additional internal deformation. Thus, dominant sheets, which developed in regions of high basement dip and experienced little internal deformation at the outset of their emplace-

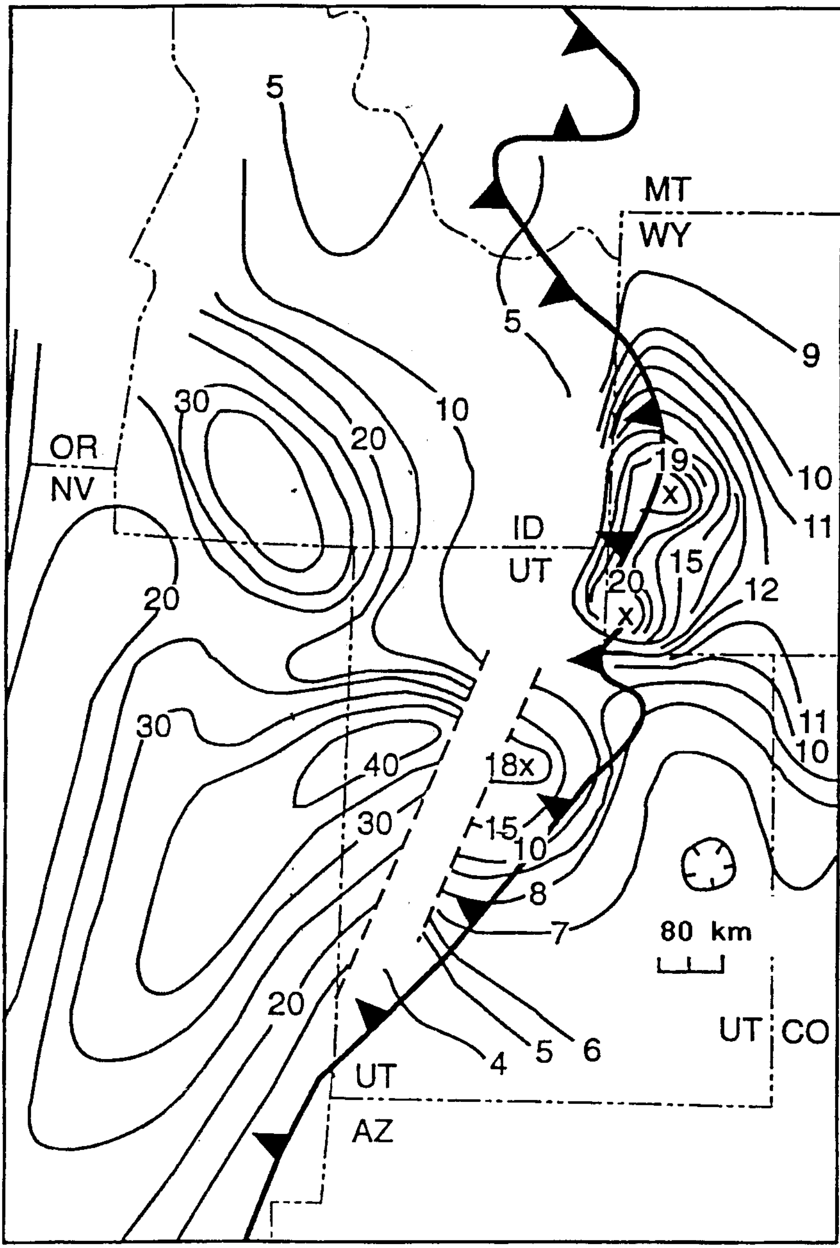
5
MT
WY
5
9
30
10
20
OR
NV
10
19
X
11
ID
UT
15
20
20
12
X
30
11
10
40
18x
30
15
10
8
7
80 km
20
4
5
6
UT
CO
UT
AZ

Figure 15

ment, may deform internally at later stages in an orogeny. This deformation may take the form of penetrative fabrics or imbrication. The need for this subsequent deformation is dependent on the degree of foreland basement subsidence accompanying thrust-belt advance.

The balance between erosion rates and foreland subsidence should influence the rate of thrust belt advance. If erosion rates are less than uplift rates, taper may become supercritical and lead to the accretion of additional frontal thrust sheets. Thrust belt advance would be accompanied by a growth in thrust belt width. If erosion keeps pace with thrusting, the thrust belt would advance at a steady state width. Should erosion exceed subsidence, internal deformation would have to increase, and the thrust belt might actually retreat or decrease in width.

VALIDITY OF THE CRITICAL-WEDGE MODEL

Boyer and Geiser (1987) argued that synchronous thrusting, out-of-sequence thrusting, and duplex faulting should operate to maintain critical taper in thrust belts. Woodward (1987) also maintained that the model requires high internal strains. Consequently, the frequent presence of low internal strains and lack of out-of-sequence thrusting would appear to reflect shortcomings in the critical wedge model (Woodward, (1987). However, by entering the wedge shape of sedimentary prisms into area balance models, I have shown that strains need not be as high as previously thought. Although there are perhaps valid criticisms of the critical-wedge model (Woodward, 1987; Price, 1988; Bombolakis, 1994), the frequent lack of penetrative internal deformation and paucity of other taper building mechanisms does not in and of itself diminish the credibility of the model. On the other hand, the utility of the critical-wedge model in explaining structural variation in thrust belts does not constitute proof of the model. The validity of the critical-wedge model needs to be evaluated further and the effect of stratigraphic taper (basin geometry) should be given equal weight with other factors, including material properties and fluid pressures within and along the base of the thrust wedge.

CONCLUSIONS

The critical wedge model of Davis, Suppe, and Dahlen (1983) can be applied to explain structural variation and kinematic evolution in thrust

Fig. 15. Paleozoic basin taper (dip on basement) may have controlled the position of thrust belt advance and the loci of synorogenic depocenters within the Idaho-Utah-Wyoming thrust belt. Contours in western Wyoming (WY) and central and eastern Utah (UT) are isopachs of synorogenic Cretaceous sedimentary rocks. Contours in western Utah, Nevada, and Idaho reflect thicknesses of Paleozoic sedimentary rocks. Depocenters of Cretaceous basins are indicated by "X." Thicknesses in thousands of feet. Note that the synorogenic depocenters (Reeside, 1944) lie due east of the Paleozoic depocenters (Peterson, 1977). Thrust belt advance would have been the greatest in areas of highest basement dip, thus producing the prominent thrust salients and corresponding synorogenic depocenters.

belts. The pre-deformational dip on basement defines the primary taper of a sedimentary basin. All other mechanical factors being equal, primary taper will control the spacing of thrusts, magnitude of internal shortening within the thrust wedge, the width of thrust belts, and rates of thrust belt advance.

Thrust spacing varies as a function of stratigraphic thickness. In basins with relatively thin stratigraphic sequences and low taper, thrusts will be more numerous and closely spaced than would be the case for thicker sequences of the same taper. The greatest variation in spacing of thrusts will occur in basins with high primary taper, since changes in thickness take place over larger distances.

Since the magnitude of critical taper varies inversely with the dip on the sole thrust, thrust belts developed in low-taper basins require greater internal deformation to attain the requisite taper. Thus, basin morphology controls the need for taper-building mechanisms, such as pressure-solution cleavage, schistosity, out-of-sequence and synchronous thrusting, and duplex faulting. Due to the convex shape of basins, thrust spacing should decrease and internal strain should increase toward the foreland. Lateral changes in basin taper will produce corresponding variation in structural geometry and kinematics.

Strain within the thrust wedge diminishes the tectonic shortening available for thrust front advance. Thrust belts developed in basins of lower taper will be narrower and experience slower thrust belt growth and advance, a greater percentage of tectonic shortening being absorbed in internal shortening to build taper.

The qualitative correlation of structural variation with predictions of the critical-wedge model does not prove the model. Such correlations simply indicate compatibility between observations and the model. However, criticisms of the critical-wedge model based on the magnitude and distribution of strain within thrust belts must take into account the influence of basin taper.

ACKNOWLEDGMENTS

I gratefully acknowledge support provided by the National Science Foundation under grants EAR-88-03623 and EAR-90-04303. I thank the reviewers of this paper, Steve Wojtal, Dan Davis, Nick Woodward, and Darrel Cowan, who helped clarify numerous technical points. I also benefited from the comments of Bob Lillie and Gautam Mitra. In addition Steve and Darrel offered numerous suggestions that improved the efficiency of presentation. Of course, they are not to be blamed for my failure to incorporate properly all their suggestions. Thrust mechanics has been an extensive area of research for the past 20 yrs, and especially in the past 10 yrs the amount of literature in this area has been overwhelming. Therefore, I apologize in advance for my certain failure to incorporate fully all the relevant literature.

Appendix 1

Derivation of Equations to Determine Average Strain within Thrust Wedge

Assuming that basins have the configuration of simple prisms, area balance equations can be derived to estimate the amount of strain rocks in the basin will experience as the sedimentary prism is deformed to a thrust prism (fig. A-1). Consider a sedimentary basin in which the dip on basement, the primary basinal taper, is β_0. The sedimentary prism has a undeformed width of l_0 and a cross-sectional area of A_0. The depth at the deepest part of the basin is h_0.

As the thrust front sweeps to the cratonward edge of the sedimentary prisms, rocks within the prism will be internally deformed to create a thrust wedge. The thrust belt has width of l', surface slope of α, and basement dip of β. In this treatment I will assume that there is no erosion and no crustal subsidence due to tectonic loading. Therefore, $\beta = \beta_0$. The area of the deformed wedge is divided into two elements: (1) A_a, above the horizontal datum; and (2) A_b, below the datum.

The areas of the sedimentary prism, A_0, and resulting thrust belt, A', are given by:

$$A_0 = h_0^2/(2 \tan \beta_0), \tag{A1-1}$$

and

$$A' = \{h_a^2(2 \tan \alpha)\} + \{h_b^2(2 \tan \beta)\}. \tag{A1-2}$$

Assuming constant area strain,

$$A_0 = A'$$

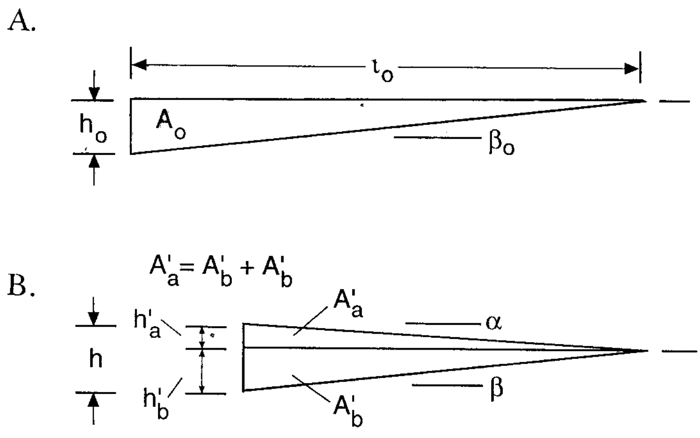

Fig. A1-1(A) A sedimentary basin of taper β_0 and area A_0 prior to deformation. The width of the basin is l_0 and the height at the "rear" of the reference wedge the basin has a depth of h_0.

(B) As the thrust front progresses across a sedimentary basin to the basin's foreland margin, the sedimentary wedge is transformed into a thrust wedge with a taper of $\alpha + \beta$. The surface topography has a dip of α. In this simple treatment, effects of tectonic loading are ignored, yielding $\beta = \beta_0$. The area of the deformed wedge is $A'_a + A'_b$, the former being the area above a horizontal datum, and the latter the area below the datum. The height at the back of the thrust wedge is $h' = h'_a + h'_b$.

App. 1 employs these geometric relations to calculate the strain created as deformation creates a thrust wedge from a sedimentary prism.

Equating (1) and (2), replacing h_a by l' tan α and h_b by l' tan β, and solving for l' yields:

$$l' = h_0\{(\tan\beta)(\tan\alpha + \tan\beta)\}^{-1/2}. \quad \text{(A1-3)}$$

Since $h_a = l' \tan\alpha$ and $h_b = l' \tan\beta$, the height above datum and depth below datum at the back of the thrust wedge are given by:

$$h_a = \{h_0 \tan\alpha\}\{(\tan\beta)(\tan\alpha + \tan\beta)\}^{-1/2}$$

and

$$h_b = \{h_0 \tan\beta\}\{(\tan\beta)(\tan\alpha + \tan\beta)\}^{-1/2}.$$

The height at the back of the thrust wedge is given by:

$$h' = h_0(\tan\alpha \cot\beta + 1)^{1/2}. \quad \text{(A1-4)}$$

The critical taper of the thrust wedge is $\tau = \alpha + \beta$. For angles $< 10°$, $\tan\tau \approx \tan\alpha + \tan\beta$. Substituting the latter relation, eqs (3) and (4) become:

$$l' \approx h_0\{(\tan\beta)(\tan\tau)\}^{-1/2} \quad \text{(A1-5)}$$

$$h' \approx h_0(\tan\tau)^{1/2}(\tan\beta)^{-1/2}. \quad \text{(A1-6)}$$

Since $l_o = h_o/\tan\beta$, the horizontal shortening and vertical stretch are:

$$H_s \approx l'/l_0 \approx (\tan\beta \cot\tau)^{1/2} \quad \text{(A1-7)}$$

and

$$V_E \approx h'/h_0 \approx (\tan\tau \cot\beta)^{1/2}. \quad \text{(A1-8)}$$

The average strain within the body of the thrust wedge is given by the ratio of the stretches:

$$AR \approx V_E/H_s \approx \tan\tau \cot\beta. \quad \text{(A1-9)}$$

Appendix 2

Derivation of Equations Dealing with Frontal Advance of Thrust Belts

If one assumes that basin morphology can be modeled in simple prismatic segments, area balance equations can be derived to predict the advance of an ensuring thrust belt. For the simplest case consider a basin in which the basin has a maximum thickness of t_c, the thickness of sediments in the foreland is t_f, and the basin is flat-bottomed (fig. A2-1).

In plane strain, a tectonic translation, d_r at the back of the thrust wedge, will sweep out an area A_s equal to the area of uplift, A_u.

$$A_s = d_r(t_c). \quad \text{(A2-1)}$$

There are three topographic segments to the orogenic belt: (1) a frontal thrust belt with a topographic dip of α_f; (2) an intermediate thrust belt with a topographic dip of α_i; and (3) a core region of plateau uplift, $\alpha = 0$. These segments have areas of A_f, A_i, and A_c, respectively. The heights at the back of the frontal thrust wedge and intermediate belt are h_f and h_c, respectively, and the widths of the frontal, intermediate, and core belts are w_f, w_i,

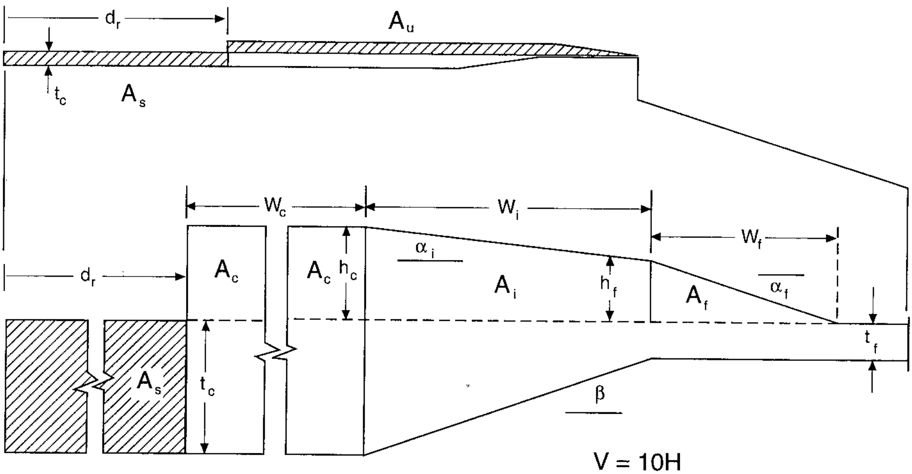

Fig. A2-1. Creation of a critically tapered thrust wedge under constraints of plane strain. The upper figure is at a scale of 1:1. The bottom figure has a vertical exaggeration of 10:1.

After a tectonic displacement of "d_r", the area of shortening, "A_s" equals area of uplift "A_u". There are three components of uplift: (1) a frontal thrust wedge of area "A_f", width "W_f", and taper angle "α_f"; (2) an internal thrust wedge of area "A_i", width "W_i", and taper angle "α_i"; and (3) the plateau uplift of the core with an area "A_c", width "W_c", and taper angle "$\alpha_c = 0$". The dip on the basement is β beneath the intermediate thrust wedge. Dips on foreland basement and bottom of the basin are zero. "t_f" is the thickness of sediments on the foreland basement and "t_c" is thickness of sediments in the basin.

For the purposes of illustration, the model is constructed with $\beta = 6°$, $t_c = 15$ km, $t_f = 4$ km, and $d_r = 250$ km. Since $\beta = 6°$, $W_i = 105$ km. Assuming a Coulomb material, from the equations of Davis and others (1983), $\alpha_f = 5.9°$, and $\alpha_i = 1.9°$, "h_f" = 7.2 km and "h_c" = 10.8 km.

and w_c. Therefore, the area of uplift is given by:

$$A_u = A_f + A_i + A_c$$
$$= \{w_f h_f/2\} + \{w_i(h_c + h_f)/2\} + \{w_c h_c\}. \quad \text{(A2-2)}$$

Since "$h_f = w_f \tan \alpha_f$" and "$h_c = w_f \tan \alpha_f + w_i \tan \alpha_i$", eq (2) becomes

$$Au = \{w_f^2 \tan \alpha_f/2\} + \{w_i(2w_f \tan \alpha_f + w_i \tan \alpha_i)/2\}$$
$$+\{w_c(w_f \tan \alpha_f + w_i \tan \alpha_i)\}. \quad \text{(A2-3)}$$

From the plane strain assumption, "$A_s = A_u$", it follows from (1) and (3) that

$$d_r(t_c) = \{w_f^2 \tan \alpha_f/2\} + \{w_i(2w_f \tan \alpha_f + w_i \tan \alpha_i)/2\}$$
$$+ \{w_c(w_f \tan \alpha_f + w_i \tan \alpha_i)\},$$

which can be rewritten as a quadratic equation in terms of "w_f":

$$(\tan \alpha_f)w_f^2 + (2w_i \tan \alpha_f + 2w_c \tan \alpha_f)w_f + (w_i^2 \tan \alpha_i)$$
$$+ (2w_c w_i \tan \alpha_i) - 2d_r(t_c) = 0. \quad \text{(A2-4)}$$

Solving for the width of the frontal thrust wedge,

$$w_f = -(w_i + w_c) + \{(w_i + w_c)^2 - [\tan \alpha_i(w_i^2 + 2w_cw_i) - 2d_rt_c] \cot \alpha_f\}^{1/2}. \quad \text{(A2-5)}$$

The width of the intermediate belt is given by

$$w_i = (t_c - t_f) \cot \beta, \quad \text{(A2-6)}$$

where β is the dip on basement. The width of the core is given by

$$w_c = w_r - d_r, \quad \text{(A2-7)}$$

where w_r is an initial reference width for the deformed core. It must be noted the w_r is somewhat arbitrary. In the calculations I have tried to identify values of w_c and d_r that are representative of many deformed belts and then back-calculated a value for w_r.

The above equations describe relations when the frontal edge of the thrust belt has passed the hinge line of the basin. In the early stages of thrust belt advance, the thrust front will lie over the basin margins with a basement dip of β. In these cases there is only one thrust wedge of constant topography, and eq (5) simplifies to:

$$w_f = -w_c + \{w_c^2 + 2d_rt_c (\cot \alpha_f)\}^{1/2}. \quad \text{(A2-8)}$$

From eqs (5), (6), (7), and (8), I set up a spreadsheet to calculate w_c, w_i, and w_f for various tectonic translations d_r and basement dips β. I assumed that thrust belts behave as the Coulomb wedge models of Davis, Suppe, and Dahlen (1983), so that $\alpha = 5.9$ to 0.66β. The basins were modeled to be 15 km deep (t_c). For various basin configurations in which β varied laterally in increments of 1°, I then plotted w_t, the total width of the thrust belt, versus d_r to illustrate the changing geometry of the thrust front as tectonic translation increased. The result is plotted as figure 12. Corresponding sequential cross sections (fig. 11) were prepared from the same spreadsheet calculations.

References

Bayer, K. C., 1983, Generalized structural, lithologic, and physiographic provinces in the fold and thrust belts of the United States (exclusive of Alaska and Hawaii): U. S. Geological Survey map, scale 1:2,500,000.

Beaumont, C., 1981, Foreland basins: Royal Astronomical Society Geophysical Journal, v. 65, p. 291–329.

Beutner, E. E., 1977, Causes and consequences of curvature in the Sevier orogenic belt, Utah to Montana, *in* Heisey, E. L., Lawson, D. E., Norwood, E. R., and Hale, Lyle A., editors, Rocky Mountain Thrust Belt Geology and Resources: Wyoming Geological Association, Annual Field Conference, 29th, p. 353–365.

Blackstone, D. L., Jr., and De Bruin, R. H., 1987, Tectonic map of the overthrust belt, western Wyoming, northwestern Utah, and southeastern Idaho: The Geological Survey of Wyoming, Map Series 23, scale 1:316,800.

Bombolakis, E. G., 1994, Applicability of critical wedge theories to foreland belts: Geology, v. 22, no. 6, p. 535–538.

Boyer, S. E., 1986, Geometric evidence for simultaneous, rather than sequential, movement on major thrusts; implications for duplex development: Geological Society of America Abstracts with Programs, v. 18, p. 549.

——— 1991, Sedimentary basin taper as a factor controlling structural variation in thrust belts: Geological Society of America, Abstracts with Programs, v. 23, no. 1, p. 10.

——— 1992, Geometric evidence for synchronous thrusting in the southern Alberta and northwest Montana thrust belts, *in* McClay, K. R., editor, Thrust Tectonics: London, Chapman & Hall, p. 377–390.

——— 1993, Geometry and sequential evolution of thrust systems in the thrust belt of northwest Montana: Support for the critical-wedge model: Geological Society of America, Abstracts with Programs, v. 25, no. 5, p. 12–13.

Boyer, S. E., and Elliott, D., 1982, Thrust systems: American Association of Petroleum Geologists Bulletin, v. 66, p. 1196–1230.

Boyer, S. E., and Geiser, P. A., 1987, Sequential development of thrust belts: implications for mechanics and cross section balancing: Geological Society of America Abstracts with Programs, v. 19, no. 7, p. 597.
Bucher, W. H., 1956, The role of gravity in orogenesis: Geological Society of America Bulletin, v. 67, p. 1295–1318.
Cadell, H. M., 1888, Experimental researches in mountain building: Royal Society of London Transactions, v. 35, Part I, no. 7, p. 337–357.
Calassou, S., Larroque, C., and Malavieille, J., 1993, Transfer zones of deformation in thrust wedges: an experimental study: Tectonophysics, v. 221, p. 325–344.
Chapple, W. M., 1978, Mechanics of thin-skinned fold-and-thust belts: Geological Society of America Bulletin, v. 89, p. 1189–1198.
Colletta, B., Letouzey, J., Pinedo, R., Ballard, J. F., and Balé, P., 1991, Computerized X-ray tomography analysis of sandbox models: Examples of thin-skinned thrust systems: Geology, v. 19, p. 1063–1067.
Coogan, J. C., 1993, Structural evolution of piggyback basins in the Wyoming-Idaho-Utah thrust belt, *in* Link, P. K., Kuntz, M. A., and Platt, L. B., editors, Regional Geology of Eastern Idaho & Western Wyoming: Geological Society of America Memoir 179, p. 55–81.
Crider, J., and Boyer, S. E., 1993, Evidence for synchronous thrusting in the northern Sawtooth Range, Montana: Geological Society of America Abstracts with Programs, v. 25, no. 5, p. 25.
Crosby, G. W., 1969, Vertical movements and isostacy in western Wyoming overthrust belt: American Association of Petroleum Geologists Bulletin, v. 52, p. 2000–2015.
Dahlen, F. A., 1984, Noncohesive critical coulomb wedges: An exact solution: Journal of Geophysical Research, v. 89, p. 10,125–10,133.
——— F. A., 1988, Mechanical energy budget of a fold-and-thrust belt: Nature, v. 331, p. 335–337.
——— F. A., 1990, Critical taper model of fold-and-thrust belts and accretionary prisms: Annual Review of Earth and Planetary Sciences, v. 18, p. 55–99.
Dahlen, F. A., and Suppe, J., 1988, Mechanics, growth, and erosion of mountain belts, *in* Clark, S. P., Jr., Burchfiel, B. C., and Suppe, J., editors, Processes in Continental Lithospheric Deformation: Geological Society of America Special Paper 218, p. 161–178.
Dahlen, F. A., Suppe, J., and Davis, D., 1984, Mechanics of fold-and-thrust belts and accretionary wedges: cohesive Coulomb theory: Journal of Geophysical Research, v. 89 (B12), p. 10,087–10,101.
Davis, D. M., and Engelder, T., 1985, The role of salt in fold-and-thrust belts: Tectonophysics, v. 119, p. 67–88.
Davis, D. M., Suppe, J., and Dahlen, F. A., 1983, Mechanics of fold-and-thrust belts and accretionary wedges: Journal of Geophysical Research, v. 88, p. 1153–1172.
De Jong, K. A., and Scholten, R., 1973, Gravity and Tectonics: New York, John Wiley & Sons, 502 p.
Delphia, J., and Bombolakis, E. G., 1988, Sequential development of a frontal ramp, imbricates, and a major fold in the Kemmerer region of the Wyoming thrust belt, *in* Mitra, G., and Wojtal, S., editors, Geometires and Mechanisms of Thrusting, with Special reference to the Appalachians: Geological Society of America Special Paper 222, p. 207–222.
Dixon, J. M., and Liu, S., 1992, Centrifuge modelling of the propagation of thrust faults, *in* McClay, K. R., Thrust Tectonics: London, Chapman & Hall, p. 53–69.
Dixon, J. S., 1982, Regional structural synthesis, Wyoming Salient of western overthrust belt: American Association of Petroleum Geologists Bulletin, v. 66, p. 1560–1580.
Elliott, D., 1976, The motion of thrust sheets: Journal of Geophysical Research, v. 81, p. 949–963.
Emerman, S. H., and Turcotte, D. L., 1987, A fluid model for the shape of accretionary wedges: Earth and Planetary Science Letters, v. 63, p. 379–384.
Fletcher, R. C., 1989, Approximate analytical solutions for a cohesive fold-and-thrust wedge: Some results for lateral variation in wedge properties and for finite wedge angle: Journal of Geophysical Research, v. 94, no. B8, p. 10,347–10,354.
Geiser, P. A., 1988a, Mechanisms of thrust propagation: some examples and implications for the analysis of overthrust terranes: Journal of Structural Geology, v. 10, p. 829–845.
——— 1988b, The role of kinematics in the construction and analysis of geological cross sections in deformed terranes, *in* Mitra, G., and Wojtal, S., editors, Geometry and Mechanisms of Faulting with Special reference to the Appalachians: Geological Society of America Special Paper 222, p. 47–75.

Geiser, P. A., and Engelder, T., 1983, The distribution of layer parallel shortening fabrics in the Appalachian foreland of New York and Pennsylvania: evidence for two-non-coaxial phases of the Alleghanian orogeny, *in* Hatcher, R. D., Williams, H., and Zeitz, I., editors, Contributions to the Tectonics and Geophysics of Mountain Chains: Geological Society of America Memoir 158, p. 161–175.
Goff, D., and Wiltschko, D. V., 1992, Stresses beneath ramping thrusts: Journal of Structural Geology, v. 14, p. 437–450.
Grubbs, K. L., and van der Voo, R., 1976, Structural deformation of the Idaho-Wyoming overthrust belt (USA) as determined by Triassic paleomagnetism: Tectonophysics, v. 33, p. 321–336.
Gwinn, V., 1967, Curvature of marginal folded belts flanking major mountain ranges: accentuated or caused by lateral translation of epidermal stratified cover?: Geological Society of America Abstracts with Program, New Orleans, v. 78, p. 87.
Harris, S. A., 1957, The tectonics of Montana as related to the Belt Series: Billings Geological Society, Annual Field Conference Guidebook, 8th, p. 22–33.
Harrison, J. E., Griggs, A. B., and Wells, J. D., 1974, Tectonic features of the Precambrian Belt Basin and their influence on post-Belt structures: U.S. Geological Survey Professional Paper 866, 15 p.
Hayes, K. H., 1977, A discussion of the geology of the southeastern Canadian Cordillera and its comparison to the Idaho-Wyoming-Utah fold and thrust belt, *in* Hill, J. G., editor, Geology of the Cordilleran Hingeline–1976 Symposium: Rocky Mountain Association of Geologists, p. 59–82.
Horberg, L., Nelson, V., and Church, V., 1949, Structural trends in central Wyoming: Geological Society of America Bulletin, v. 60, p. 183–216.
Hubbert, M. K., and Rubey, W. W., 1959, Role of fluid pressure in mechanics of overthrust faulting: Geological Society of America Bulletin, v. 70, p. 115–166.
Huiqi, L., McClay, K. R., and Powell, D., 1992, Physical models of thrust wedges, *in* McClay, K. R., editor, Thrust Tectonics: London, Chapman & Hall, p. 71–81.
Jaumé, S. C., and Lillie, R. J., 1988, Mechanics of the Salt Range-Potwar Plateau Pakistan: A fold-and-thrust belt underlain by evaporites: Tectonics, v. 7, p. 57–71.
Jordan, T., 1981, Thrust loads and foreland basin evolution, Cretaceous, western United States: American Association of Petroleum Geologists Bulletin, v. 15, p. 2506–2520.
Kopania, A. A., 1983, Deformation consequences of the impingement of the foreland and northern thrust belt, eastern Idaho and western Wyoming: Geological Society of America Abstracts with Programs, v. 18, p. 367.
Lamerson, P. R., 1982, The Fossil Basin and its relationship the Absaroka thrust system, Wyoming and Utah, *in* Powers, R. B., editor, Geologic Studies in the Cordilleran Thrust Belt: Rocky Mountain Association of Geologists, p. 279–340.
Lawton, T. F., Boyer, S. E., and Schmitt, J. G., 1994, Influence of inherited taper on structural variability and conglomerate distribution, Cordilleran fold and thrust belt, western United States: Geology, v. 22, no. 4, p. 339–342.
Lillie, R. J., Johnson, G. D., Yousuf, M., Zamin, A. S. H., and Yeats, R. S., 1987, Structural development within the Himalayan foreland fold-and-thrust belt of Pakistan, *in* Beaumont, C., and Yankard, A. J., editors, Sedimentary Basins and Basin-Forming Mechanisms: Canadian Society of Petroleum Geologists, Memoir 12, p. 379–392.
Liu, S., and Dixon, J. M., 1991, Centrifuge modelling of thrust faulting: Structural variations along strike in fold-thrust belts: Tectonophysics, v. 188(1/2), p. 39–62.
Marshak, S., 1988, Kinematics of orocline and arc formation in thin-skinned orogens: Tectonics, v. 7, p. 73–86.
Marshak, S., and Wilkerson, M. S., 1992, Effect of overburden thickness on thrust belt geometry and development: Tectonics, v. 11, p. 560–566.
Marshak, S., Wilkerson, M. S., and Hsui, A. T., 1992, Generation of curved fold-thrust belts: Insight from simple physical and analytical models, *in* McClay, K. R., editor, Thrust Tectonics: London, Chapman & Hall, p. 83–92.
Mitra, G., 1993, Strain variation in thrust sheets of the Sevier fold-and-thrust belt, Idaho-Utah-Wyoming: Implications for section restoration and wedge taper evolution: Geological Society of America Abstracts with Programs, v. 25, no. 5, p. 123.
Mitra, G., Hull, J. M., Yonkee, W. A., and Protzman, G. M., 1988, Comparison of mesoscopic and microscopic deformational styles in the Idaho-Wyoming thrust belt and the Rocky Mountain foreland, *in* Schmidt, C. J., and Perry, W. J., Jr., editors, Interaction of the Rocky Mountain Foreland and the Cordilleran Thrust Belt: Geological Society of America Memoir 171, p. 119–141.

Mudge, M. R., and Earhart, R. L., 1983, Bedrock geologic map of part of the northern Disturbed Belt, Lewis and Clark, Teton, Pondera, Glacier, Flathead, Cascade, and Powell Counties, Montana: U.S. Geological Survey Miscellaneous Investigations Series, Map I-1375, 1:125,000.
Mugnier, J. L., and Vialon, P., 1986, Deformation and displacement of the Jura cover on its basement: Journal of Structural Geology, v. 8, p. 373–387.
Mulugeta, G., 1988, Modelling the geometry of Coulomb thrust wedges: Journal of Structural Geology, v. 10, p. 847–859.
Mulugeta, G., and Koyi, H., 1987, Three-dimensional geometry and kinematics of experimental piggyback thrusting: Geology, v. 15, p. 1052–1056.
——— 1992, Episodic accretion and strain partitioning in a model sand wedge: Tectonophyics, v. 202, p. 319–333.
Nickelsen, R. P., 1972, Attributes of rock cleavage in some mudstones and limestones of the Valley and Ridge province of Pennsylvania: Pennsylvania Academy of Science Proceedings, v. 46, p. 107–112.
——— 1979, Sequence of structural stages of the Alleghany Orogeny, at the Bear Valley Strip Mine, Shamokin, Pennsylvania: American Journal of Science, v. 279, p. 225–271.
Peterson, J. A., 1977, Paleozoic self-margins and marginal basins, western Rocky Mountains-Great Basin, United States; *in* Heisey, E. L., Norwood, E. R., Wach, P. H., and Hale, L. A., editors, Rocky Mountain Thrust Belt: Geology and Resources: Wyoming Geological Association, p. 135–153.
Platt, J. P., 1988, The mechanics of frontal imbrication: a first order analysis: Geologisches Rundschau, v. 77, no. 2, p. 577–589.
Price, R. A., 1973, Large-scale gravitational flow of supercrustal rocks, southern Canadian Rockies, *in* De Jong, K. A., and Scholten, R., editors, Gravity and Tectonics: New York, John Wiley & Sons, p. 491–502.
——— 1988, The mechanical paradox of large overthrusts: Geological Society of America Bulletin, v. 100, p. 1898–1908.
Protzman, G. M., and Mitra, G., 1985, Emplacement history of a thrust sheet based on analysis of pressure solution cleavage and deformed fossils: Geological Society of America Abstracts with Programs, v. 17, p. 694.
Puigdefàbregas, C., Muñoz, J. A., and Vergés, J., 1992, Thrusting and foreland basin evolution in the southern Pyrenees, *in* McClay, K. R., editor, Thrust Tectonics: London, Chapman & Hall, p. 247–254.
Reeside, J. B., 1944, Map showing thickness and general character of the Cretaceous deposits in the western interior of the United States: U.S. Geological Survey Oil and Gas Investigations Preliminary Map 10, Scale 1″ = 220 miles.
Rodgers, John, 1970, The Tectonics of the Appalachians: New York, Wiley, 271 p.
Royse, F., Jr., 1993, An overview of the geologic structure of the thrust belt in Wyoming, northern Utah, and eastern Idaho, *in* Snoke, A. W., Steidtmann, J. R., and Roberts, S. M., editors, Geology of Wyoming: Geological Survey of Wyoming Memoir No. 5, p. 272–311.
Royse, F., Jr., Warner, M. A., and Reese, D. L., 1975, Thrust belt structural geometry and related stratigraphic problems, Wyoming-Idaho-northern Utah, *in* Bolyard, D. W., editor, Symposium on Deep Drilling Frontiers in the Central Rocky Mountains: Rocky Mountain Association of Geologists, p. 41–54.
Stockmal, G. S., 1983, Modeling of large-scale accretionary wedge deformation: Journal of Geophysical Research, v. 88, no. B10, p. 8271–8287.
Suppe, J., and Wittke, J. H., 1977, Abnormal pore-fluid pressure in relation to stratigraphy and structure in the fold-and-thrust belt of northwestern Taiwan: Petroleum Geology of Taiwan, v. 14, p. 11–24.
Thomas, W. A., 1990, Controls on locations of transverse zones in thrust belts: Eclogae geologicae Helvetiae, v. 83, no. 3, p. 727–744.
Vergés, J., and Muñoz, J. A. 1990, Thrust sequences in the Southern Central Pyrenees: Bulletin de la Société géologique de France, v. 8, p. 265–271.
Winston, D., 1986, Sedimentation and tectonics of the Middle Proterozoic Belt Basin and their influence on Phanerozoic compression and extension in western Montana and northern Idaho, *in* Peterson, J. A., editor, Paleotectonics and Sedimentation in the Rocky Mountain Region, U.S.: American Association of Petroleum Geologists Memoir 41, p. 87–118.

Woodward, N. B., 1987, Geological applicability of critical-wedge thrust-belt models: Geological Society of America Bulletin, v. 99, p. 827–832.

——— 1988, Primary and secondary basement controls on thrust sheet geometries, *in* Schmidt, C. J., and Perry, W. J., Jr., editors, Interaction of the Rocky Mountain Foreland and Cordilleran Thrust Belt: Geological Society of America Memoir 171, p. 353–366.

Woodward, N. B., and Rutherford, E., Jr., 1989, Structural lithic units in external orogenic zones: Tectonophysics, v. 158, p. 247–268.

Yoos, T. R., Potter, C. J., Thigpen, J. L., and Brown, L. S., 1991, The Cordilleran foreland thrust belt in northwestern Montana and northern Idaho from COCORP and industry seismic reflection data: American Association of Petroleum Geologists Bulletin, v. 75, no. 6, p. 1089–1106.

Zhao, W. L., Davis, D. M., Dahlen, F. A., and Suppe, J., 1986, Origin of convex accretionary wedges: evidence from Barbados: Journal of Geophysical Research, v. 91, p. 10,246–10,258.